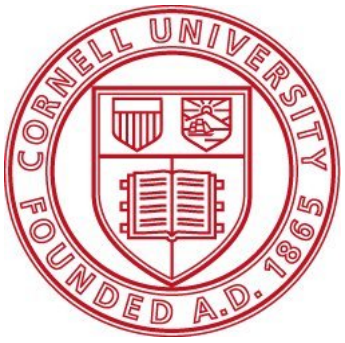

Cornell MineSweeper

Spring 2007
Technical Report

Cornell MineSweeper: Semester Overview

Vikas Reddy, Project Manager, ve23@cornell.edu

***Abstract*—Cornell MineSweeper is a student-found, student-led team developing an autonomous solution for humanitarian demining. The team has currently completed its frame design and has finalized most of the power and control systems along with the sensors for obstacle and lane detection. This overview report briefly summarizes the work accomplished in Spring 2007 and also describes the team's future direction.**

I. Introduction

CORNELL MINESWEEPER was founded in Fall 2006 to develop autonomous robots for landmine detection. The team started with 42 members and is currently 33 members strong. It was initially structured under 5 sub-groups – Frame Design, Power and Controls, Sensors, Computing and Business.

The primary goals for this semester were as follows:

- Complete design of the frame, drivetrain and suspension
- Fabricate and Test RF control
- Decide on Power source and management
- Shortlist potential landmine detection technologies
- Set up SIMBAD robot simulator
- Complete Website and Sponsorship Pamphlet

II. Specifications

The specifications for the robot were taken from the requirements of the Intelligent Ground Vehicle Competition and from literary research regarding landmine detection. It was decided that an all-terrain robot with on-board image processing, GPS and IMU powered by a battery would be a very adaptable solution. Specs for each of the components were drawn up by the respective groups except for the GPS which was bought from U-blox and the IMU which was donated by Kionix. Also, the competition required that each robot have an emergency stop button on the robot along with a wireless E-stop. Thus, the primary tasks were that of designing the frame, power solution and wireless E-stop on the hardware side and image processing on the software side.

Two frames were designed with different batteries, suspension and drivetrain and the overall concept is described in the following sections.

III. Robot Concept V1.0

The first concept is the low cost solution which uses a lead acid battery and two motors to propel the robot. It has a six wheeled all-wheel drivetrain which provides it good traction on all terrain conditions. The two motors transmit equal torque to all wheels via a belt-pulley drive and the robot is steered via skid steer with the each motor controlling three wheels. The specifics of the drivetrain and motor control are described in the drivetrain report and control systems report respectively. Figure 1 shows the rendered image of v1.0

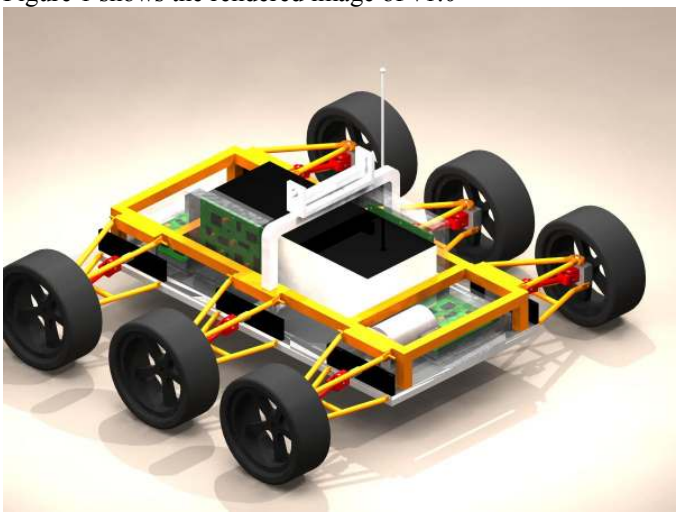

Fig.1. Rendering of Concept v1.0

The critical components of this chassis were the A-arm suspension, the belt-pulley drivetrain and the precise alignment of the three wheels on each side to ensure proper steering. Since the primary objective of the robot was to lower costs, it is critical that there are very high tolerances for machining and assembling components.

The other limitation of this chassis was the lack of feedback control for each wheel, making it harder to detect, say, if the robot is stuck in a mud pit and needs more power/torque for the front wheels. Also, using a 25kg lead acid battery to carry a payload of less than 20kgs was highly non-optimized.

Thus, it was decided to embark on a new design to fix the flaws of v1.0. Also, CU Snake Arm donated six Faulhaber 2342CR motors which channeled the design process in that direction.

IV. Robot Concept V2.0

This concept is an optimized version of v1.0 featuring an innovative in-wheel motor design and a rocker-bogie suspension. The design also incorporates lighter and more efficient, Nickel-Cadmium (Ni-Cd) batteries which only weigh 6kgs for a 240W power output. See Fig.2.

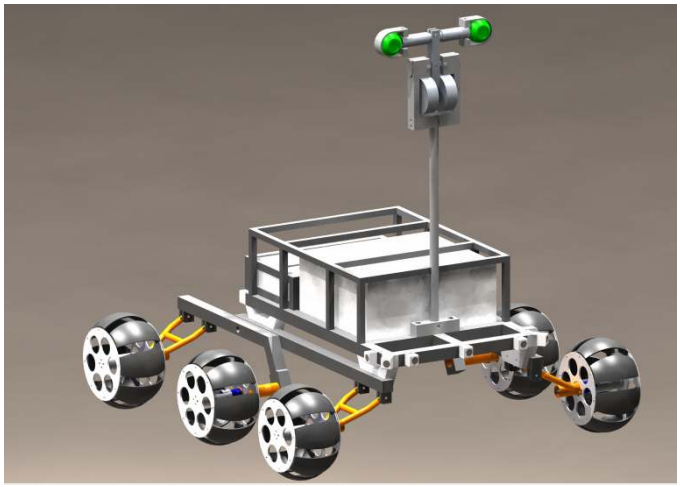
Fig.2: Initial Rendering of Concept v2.0

It features a six wheel all-wheel drive with feedback control on each wheel giving the robot greater control and steering.
The rocker-bogie suspension is the same concept used in the Mars Rovers and allows the robot to traverse obstacles twice the diameter of the wheel, giving the robot an effective obstacle clearance of 12in.
This chassis uses Maxbotix ultrasonic sensors along with stereocameras for obstacle detection. The ultrasonic sensors are controlled by a Atmega128 microcontroller while the stereocameras are controlled by a Gumstix processor (exact specs to be determined after testing).
The Faulhaber motors are DC brushed motors providing easy control via a H-bridge. Each of these motors has an optical encoder attached to provide velocity feedback to the motor controllers, thus providing 6 channels of control, all handled by the Atmega128.
This design is modular in the sense that the wheels, suspension, sensors and the casing are all independent of each other, allowing for easy upgrades and part swaps.
Thus, Concept v2.0 is a far more superior chassis design and has been chosen as the first platform. The exact specifications can be found in the Structures team report.

V. Landmine Detection Sensors

The Power team switched roles this semester and focused on the selection of the landmine detection sensors. After a thorough literary review, the team recommends testing out Acoustic Phased Arrays and an EMI Array. Refer to the Power team paper for details.

VI. MineSweeper System

With the chassis design complete, the next step is the implementation of the chassis for landmine detection. The current idea is to use a swarm of robots to scan for landmines in parallel with each robot communicating to the field computer, its current location, the landmine location and so on. As a proof of concept, the team will design and build another robot along with a base station and establish communication amongst each other. Eventually, the team will enable the robots to communicate with each other to test the benefits of cooperative robotics.

VII. Timeline

Summer 2007	Complete fabrication of Chassis 1
Fall 2007	Design Chassis 2, Base Station. Prepare Chassis 1for IGVC
Winter 2007	Field trip to Cambodia
Spring 2008	Fabricate Chassis 2 and Base Station. Test all.
Summer 2008	Compete in IGVC

VIII. Conclusion

The team accomplished most of its tasks this semester, but it needs to increase its pace of progress. To optimize team operations, all teams will be merged and divided into Chassis 1, Chassis 2, Base Station and Admin groups to enable better communication and lesser delays. Also, the team will actively source for lab space to provide a more unified working environment.
Funding wise, the team has met its current requirements and will continue to source for more sponsors.
The field trip to Cambodia in Winter 2007 will be a thorough study of the design requirements for a realistic landmine detection system.

Cornell MineSweeper: Computing

Justin Besant, Griffin Dorman, Nolan Leung, Stephen Milhone, Daniel Zuo

***Abstract*— The Cornell University Minesweeper Computer Science team was formed to develop and oversee the artificial intelligence of the minesweeper robot. Currently, the team's goals are to develop and simulate a navigation algorithm and to obtain the appropriate computing hardware. This report illustrates the team's progress and its future plans.**

I. Introduction

THE computing team worked in two different phases: from the beginning of the year up to the BOOM presentation the entire team focused on developing a simulation of our path finding algorithm in Simbad. Following the demonstration the team was divided into two sections. One group focused on developing the navigation algorithm as well as the simulator, while the other researched a computing hardware setup for the Minesweeper robot.

II. Path Finding

One of the major focuses of this semester was selecting and implementing an efficient path finding algorithm. The requirements for the IVGC competition stated that our robot must be able to follow a path and avoid any obstacles in the path. A* is an efficient and robust search algorithm capable of calculating the shortest path to a known goal given an accurate description of the terrain.

The main requirement for any path finding algorithm is an accurate graph of the surrounding area containing all possible nodes and edges. A* computes a path given a starting point and destination. At each iteration, A* will look at the adjacent nodes that is estimated to be part of the shortest path to the destination. The estimation is found by summing the shortest known path to the current node and a heuristically calculated distance from the current node to the destination.

III. A*

Our current implementation of A* relies on a matrix representing the current environment, where the nodes are represented as cells in the matrix, and edges are implicitly assumed to be between adjacent cells with weights being a weighted average between two cells. The edge weights are the product of the Euclidian distance between the two nodes and the next node's weight. Node weights signify expected difficulty in traveling through the node, where high weights indicate harder traversal and are avoided. This decision was made to account for anticipate errors in sensor data and its interpretation.

It is common in implementations of the A* algorithm to use two lists to keep track of the portion of the map already analyzed. The first list is called the "open" list, which stores the nodes that may potentially be the active node. Our implementation used a priority queue, ordered by the estimated shortest path to the destination from the start position, containing the given node. For each iteration, the active node is selected by removing the node with the shortest estimated path, since that node will have the greatest potential for being on the shortest path. The second list is the "closed" list, which stores all nodes that have been active. Our implementation of the closed list used a matrix of equal dimensions to the map. The elements of the list are initially all null, and when a node is added to the list, its corresponding location in the matrix is filled.

The current heuristic used to estimate the distance to the destination from a given node is simply the Euclidean distance. Since this gives the distance assuming a best case scenario, it is always an underestimation. For the purposes of testing, an underestimation was preferred because this guarantees that the shortest path is found. However, for practical reasons, the heuristic should overestimate the distance to the destination, because this is significantly more efficient and the path found will still be close to optimal.

Each iteration of A* is centered around an active node. The first active node is always the start location. Subsequent active nodes are found by removing the node with greatest priority on the open list. Once the active node is selected, it is

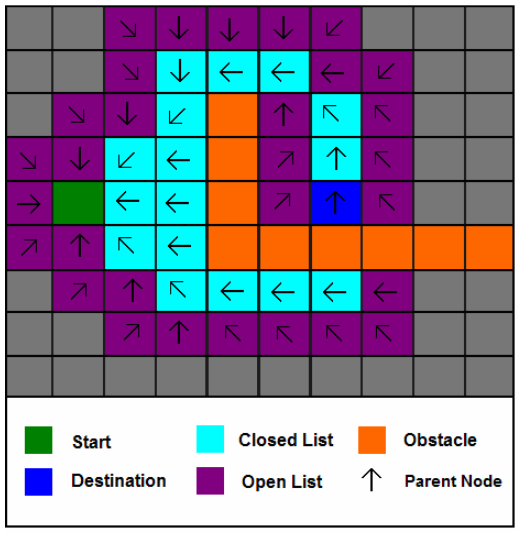

Fig. 1: An example of a completed path calculated with A.*

moved to the closed list, and all adjacent nodes that are not already on the closed list are added to the open list. Every time a node is added to the open list, it stores the node from which it came. If an adjacent node is already on the open list, and its

current estimated shortest path is longer than its estimated shortest path including the current node, the pointer its to preceding node is updated. When the active node is the destination, the algorithm halts and traces backwards to find the path. In a binary implementation of A* (where nodes are marked purely as passable or impassable), it is possible that no feasible paths exist, which is indicated by the open list being empty. However, our current implementation does not allow a node to be marked as strictly impassable, only highly undesirable.

To anticipate the limited information available about the environment, our algorithm assumes that only data pertaining to the area around the current location is given. Hence the algorithm only analyzes at a small fraction of the entire map, and views the rest of the environment as highly undesirable until it actually receives data. If the destination is not located within the area for which information is available, a temporary goal will be found via a heuristic. The algorithm will attempt to head towards that goal and in the process move the robot towards the final goal. New data will then be available afterwards, and based on the new information, a new heuristic goal will be selected and a new partial path will be found. This repeats until the information about the destination is found, at which point the algorithm will find the path to the destination.

IV. Simbad

To simulate an environment to test the A* algorithm, the computing team decided to create an environment with Simbad (http://simbad.sourceforge.net/). By using Simbad, an environment can be created with randomly placed objects and robots that are able to keep track of information like their position, speed, and angle. This information, along with a known representation of the world, is enough to perform path finding using A*.

The environment used to test A* was created by generating boxes and placing them randomly across the map. Next, the robot was spawned at a random location, and awaited user input for its destination. Every frame, Simbad prompts the robot to perform an action that will lead towards the destination. To simulate a potential change in the world, a new path is calculated by A* every ten frames. The path that A* returns a list of nodes to travel to in sequential order. The robot will move towards the first node in the path, and upon reaching it, will turn to face the next node, and proceed to that node.

To simulate a lack of data for A*, a mini-map is generated each time a new path is calculated with A*. This mini-map is a quarter of the entire world, with the robot in the center of the mini-map. On cases where the mini-map does not contain the actual destination, a waypoint is found that is part of a straight line towards the destination, but found inside the mini-map. In most cases, the waypoint is not reached before a new path is calculated on a new mini-map. During the calculation of a new path, A* has no information except for what is provided by the mini-map.

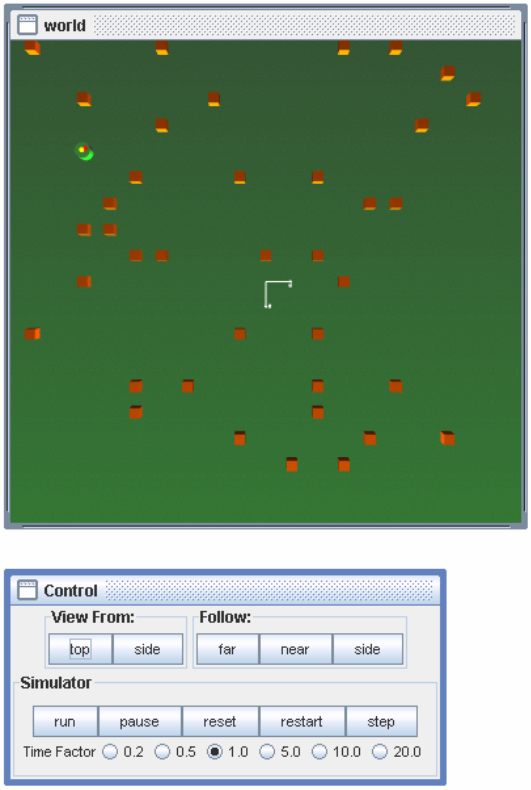

Figure 2: An example of a Simbad generated environment

Although Simbad provides a method of testing A*, the environment that can be generated is severely limited. Simbad is only able to produce even terrain, leading to a simplistic model to test A*. Another concern is Simbad's lack of support for inserting obstacles into the world, causing simple obstacles that cannot vary in shape. Lastly, Simbad gave us perfect information regarding the world, and did not account for possibly inaccurate sensor data or a lack of data.

V. Hardware

There are two main options for the computing hardware; either a stripped down laptop or embedded computer could be used. Since an embedded computer is typically less costly than a laptop, if we purchased an embedded computer, we could use the extra money to buy more sophisticated cameras.

For the embedded processor, we recommend the Verdex XL6P by Gumstix. It has extremely low power consumption at approximately 1.0 watts and is only 80mm x 20mm. Additionally, it can be operated in temperatures ranging from 25C to 85C. The Verdex XL6P sells for $169 and comes with a 600Mhz processor with 128MB RAM and 32MB flash. It runs on Linux 2.6 and supports C, sh, C++, awk, Java, Perl, Python, and TCL. Most Linux programs can be run on the Verdex without modification.

Since the embedded processor is so inexpensive, the team could use the leftover funds to purchase two advanced cameras. We recommend the CMUCam1. This camera already does image processing on board and outputs processed data. With this camera, the image processing team would not need to write nearly as much code. The camera outputs 80x143 pixels at 17 frames per second. Two of these will cost $218.

Unfortunately, an embedded processor will require a steeper learning curve than a traditional laptop processor. Some Linux programs may not necessarily work and the Computing team will need to modify code. For this reason, we alternatively recommend a low-end laptop. The lowest priced laptops generally cost about $500 and will carry a processor similar to a 1.5Ghz Celeron M with 512 MB RAM. Although it will be easier to implement the robot with a stripped-down laptop, we will be buying more components than we will need, and the laptop will consume approximately 35 to 45 watts.

VI. Future Goals

The following are the goals for the Computing Team during Fall 2007:

- Write our navigation algorithms in C
- Test our navigation algorithms with sensor input
- Perform field testing with conditions similar to IVGC competition
- Continue research on navigation

VII. Conclusion

During Spring 2007, the Computing Team focused on the implementation of A*, simulation using Simbad, and hardware research. Although the team did not perform field tests with our navigation algorithms, the team is ready to begin testing and enhancing path finding algorithms with sensor input.

Cornell MineSweeper: Image Processing

Tonislav Ivanov, Siddharth Gauba

***Abstract*—The Minesweeper Image Processing Team is responsible for the development of line detection for the purpose of the IGVC competition and also the development of an obstacle matrix. In Spring 2007, much of the emphasis was to develop a system for line detection, and it was done using the Hough feature extraction method**

I. Introduction

The overall scheme developed to detect lines has some other general components that will be desired for any image processing applications. The image form the camera is first calibrated to reduce distortion, then red saturated to remove problems occurring due to uneven lighting and shadows, after which the image is passed through an edge detector, in this case a canny edge detector. This processed, edge detected image is then processed with a Hough transform to detect prominent features such as lines.

II. The Hough Transform

A. Line Detection

The Hough transform is a mapping from the spatial image space to a parameter space corresponding to a feature that one wishes to extract. By observing which points of the parameter space have high density, one can determine where the desired feature is located in the original image. Thus, we can extract features such as straight lines using this idea.

A straight-line Hough transform finds the most probable lines that appear in an image. In this case, the most intuitive parameter space uses variables m and c, representing the slope and y-intercept of a line respectively. It is important to note that a line can be uniquely represented by a pair of m and c values. Thus, a line in the xy space is equivalent to a point in the parameter space, as shown in Fig. 1. Rewriting the equation for a line as (1), we see that a point in xy space maps to a line in mc space.

$$c = -xm + y \tag{1}$$

There are several limitations of this parameter space, namely the points become unbounded if the slope is very large. Thus, a vertical line, which is a possible in the spatial domain, becomes intractable in the mc space. A solution is to consider another parameter space based on the polar coordinates of the point defined as the intersection of the line in question and its perpendicular counterpart that passes through the origin. The parameter space is now $\rho\theta$. Again, a line in xy maps to a point in the parameter space as shown in Fig. 2. In this case, a point from xy space maps to a parabola-like curve in $\rho\theta$ space. The closed for expression is shown below in (2).

$$\rho = \frac{y\tan\theta + x}{\sqrt{1+(\tan\theta)^2}} \tag{2}$$

An example is shown in Fig. 3.

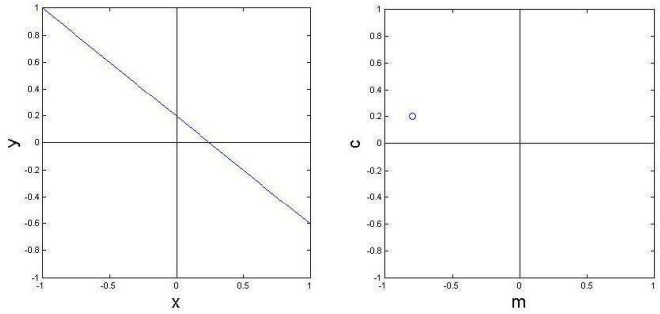

Fig. 1. Mapping from image space to parameter space. A line in xy space maps to a point in mc space.

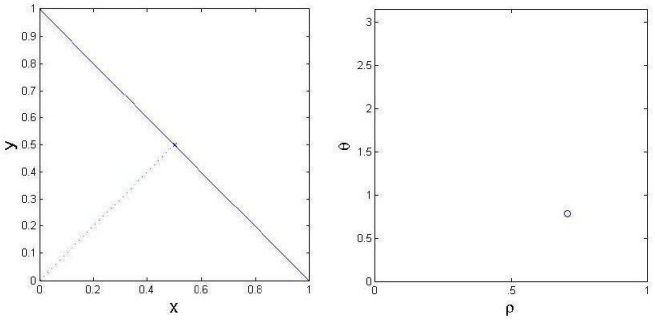

Fig. 2. Mapping from image space to parameter space. A line in xy space maps to a point in $\rho\theta$ space.

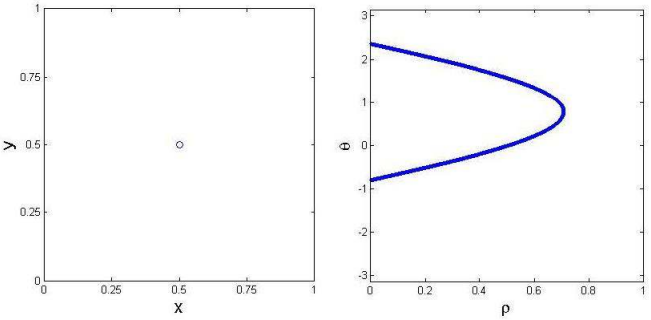

Fig. 3. Mapping from image space to parameter space. A point in xy space maps to a curve in $\rho\theta$ space.

Given a specific feature such as straight lines, the transform can serve as a method of compression by reducing the image to a small set of parameters. If only a point is given, then the Hough transform serves as an estimator of which features

Manuscript received May 19, 2007.

T. Ivanov, Siddharth Gauba are undergraduates with the Electrical Engineering Department, Cornell University, Ithaca NY 14850 USA, (email: tii2@cornell.edu sg334@cornell.edu).

would contain this point. This is very useful in navigating a robot through to fallow a straight line drawn on the floor. In particular, we can use this technique in the design for the visual system for the IGVC competition.

B. Implementation

The principles of a Hough transform can be applied to find straight lines in an image. We use an edge detector on an arbitrary picture, such as the live feed from a camera, to create a binary image. A Hough transform is applied on every pixel to form curves such as those in Fig. 3. An accumulator matrix with cells corresponding to the grid of the $\rho\theta$ space is created and every time a curve is draw, a count is added in the matrix to the cells corresponding to its pixels. This way one can track the number of times, or "votes," that a particular point in $\rho\theta$ space is a possible line in the image.

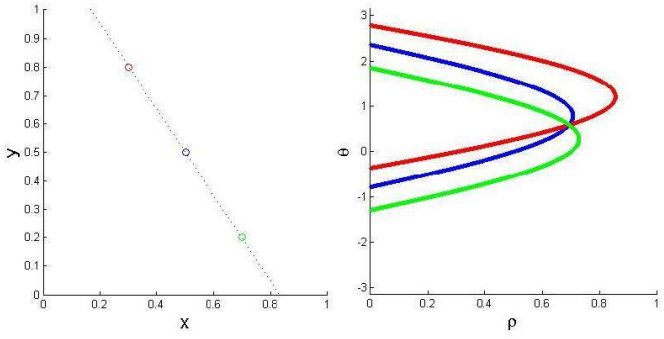

Fig. 4. The intersection of the three parabolas in $\rho\theta$ space correspond to the line that passes through the three points in the *xy* space.

Upon scanning the entire image, the points in the feature space that receive the most votes indicate the most likely lines in the image. In Fig. 4, all three curves corresponding to the given three pixels pass through a single intersection point. That point will receive a count of 3 and will correspond exactly to the line that passes through all three points.

In creating this estimator, one must consider the resolution of the accumulator matrix. A matrix with very fine resolution more accurately estimates the straight lines in the image. Although this produces a very accurate answer, the system will be very sensitive to noise since an offset from an ideal line will make it impossible for all the curves to intersect at the same point as illustrated in Fig. 5.

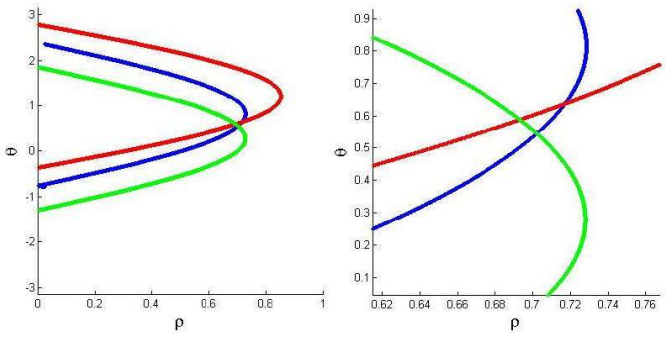

Fig. 5. The left picture shows three points that are approximately in a straight line in the image. As one zooms closer in the parameter space, it is seen that the intersection of the corresponding curves is not perfect and the result may be unstable.

This drawback can be fixed several ways. First, one could reduce the resolution of the accumulator matrix. This will create fewer possible positions to consider and increase the probability of intersection. Second, one could apply a 2-dimensional averaging filter on the accumulator matrix, which will smooth out the matrix and include the consideration of neighboring votes. It is important to note, however, that this phenomenon occurs only when there are relatively few points. In an image with many points, the problem rarely arises because enough lines will intersect to produce a correct response. Moreover, experimentation shows that recognition can be achieved even in the presence of noise and occlusion. For example, processing the images in Fig.6 , which have uneven lighting and other lines etc that could be confounding, the pre-processing and the relative robustness of the Hough transform result in a neat result as illustrated by the green lines in Fig.6.

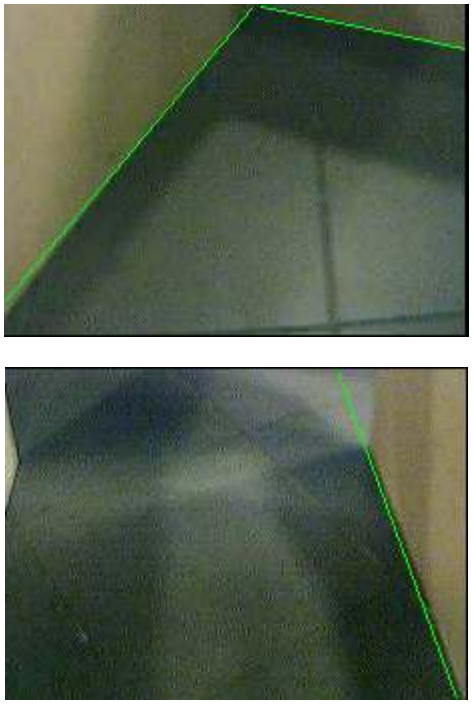

Fig. 6: Raw images and line detection processing result

C. Limitations

There are several limitations of using this method. First, it is rather brute force and therefore is computationally expensive. The algorithm is on the order of O(nmst), where n×m are the dimensions of the input image and s×t are the dimensions of the accumulator matrix. Thus, for a real-time application we need some tweaks. Past research has led to several enhancements to reduce computation time by intelligently assigning votes. Also, this algorithm becomes unstable as the number of variables in the parameter space increase. However, for lines we only need two variables; thus, the application is feasible. Finally, the Hough transform is really only successful if the input image is relatively accurate. While it is effective in a presence of random outliers and even extraneous objects, it has trouble dealing with very noisy images. In our case the assumption of high accuracy holds true, so we can apply to transform reliably. Overall, this implementation is simple and works for its purposes.

III. Conclusion

The above procedure shows an efficient process for line detection. Looking to the future, the aim will be to develop a fast and computationally less expensive method to detect the possible metric space of motion from the current spot using depth data from stereo vision. As a result, a delth map could be created which can be used by the navigation system to determine the path to follow.

References

[1] M. Sonka, V. Hlavac and R. Boyle, Image Processing, Analysis and Machine Vision, 2nd ed., Pacific Grove, CA: Brooks/Cole Publishing , 1999.

[2] Wikipedia contributors. Hough transform [Internet]. Wikipedia, The Free Encyclopedia; 2007 Mar 13, 06:01 UTC [cited 2007 Mar 13]. Available from: http://en.wikipedia.org/w/index.php?title= Hough_transform&oldid=114738751.

[3] A. Reeves. 2006. ECE 547 Lecture 14: The Hough Transforms. Cornell University.

Cornell Minesweeper: Control Systems

Siddharth Gauba, Steve Gilson, Shreya Reddy, Robert Yu

***Abstract*—This document is a discussion of the ECE team's accomplishments over the Spring 2007 semester. These were comprised of the design of a remote controlled vehicle with customized remote control functionality, emergency stop ability, and a dual control mechanism to switch between manual (remote) and automated (on-board) control.**

I. Introduction

THE semester goals for the ECE team for the Spring semester were to move from the design phase to actual procurement of parts, building, testing and integration of all the systems. The end product is a robot that can be controlled either manually or through an on-board guidance system as is being developed by a different group in the project. The entire remote control protocol is implemented in software, making it possible to augment the functionality as and when needed by simply upgrading the firmware on the requisite microcontrollers. Another feature is the asynchronous emergency stop system, that may be used to satisfy fault-tolerance as it operates on a totally different frequency and is electrically independent of the rest of the circuitry both on the remote side and the robot side, ensuring the ability to bring the robot to halt even if all systems fail, as long as the radio frequency receiver is receiving power from the battery. These functionalities were developed with an eye towards the IGVC competition as well as the practical requirements of such a robot operating in real-time situations, often used by unskilled or semi-skilled personnel.

II. PCB Design

A. Board Layout

The minesweeper will use two microcontrollers, the Atmel ATMega32 and the Atmel ATMega128. Each of these chips will sit on a custom designed circuit board. The Mega32 board connects the microcontroller to the power source and the RF receivers for the emergency stop. The same board also holds the digital logic chips to implement the emergency stop. See Figure 1.

The Mega128 microcontrollers will control the motors. They will sit on the same circuit board as the motor-driving circuits, separated by optical isolators.

B. Design and Fabrication

The Mega32 board was completed and fabricated this semester, while the Mega128 board is not yet finalized due to insufficient implementation details about any sensors needing to be interfaced or the protocol for the on-board navigation system. The boards were designed using the Orcad software library, drawn first as circuits alone in Orcad Capture, then exported to the circuit board design in Orcad Layout. Once the layout was finalized, the design was compiled in the industry-standard Gerber 274x format and sent to PCBEX (http://www.pcbex.com) for fabrication.

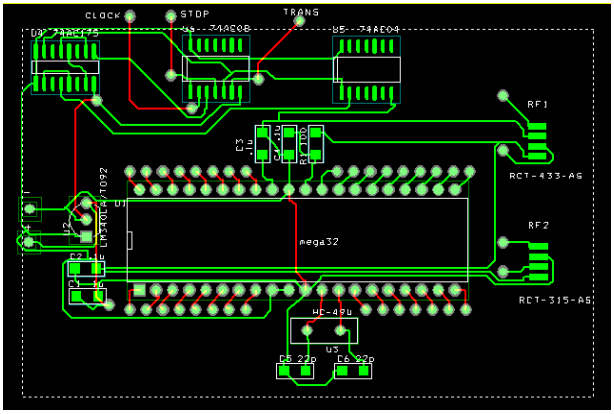

Fig 1. Final design of Mega32 board.

C. Finalization

Once the Mega32 boards arrived from PCBEX, we purchased the required resistors, capacitors and digital logic chips from Digikey (http://www.digikey.com) and soldered them to the board. We purchased five circuit boards, as that was the minimum quantity allowed and to allow for human error, but have only installed the components on one since the minesweeper will only need one remote control.

III. Emergency Stop and Remote Control

After designing the logic for the remote control and the E-Stop last semester, this semester saw the implementation and testing of the logic and the radio transmitter and receiver, as well as the ordering of the remote control that was customized in order to control the Minesweeper robot.

The logic of the controller and emergency stop was laid out and implemented onto a printed circuit board. The controller logic sends its signals to a Radiotronix 433 MHz transmitter, while the emergency stop transmits its signals over a

Radiotronix 315 MHz transmitter. There were two encoding schemes that were tried.

TABLE I
VARIABLE POWER CONTROL AT MIDDLE SETTING

Direction	Voltage
Middle (Resting)	2.37 V
Forward	2.919 V
Backward	1.758 V

TABLE II
VARIABLE POWER CONTROL AT HIGH SETTING

Direction	Voltage
Middle (Resting)	2.501 V
Forward	3.07 V
Backward	1.878 V

TABLE III
VARIABLE POWER CONTROL AT LOW SETTING

Direction	Voltage
Middle (Resting)	2.228 V
Forward	2.776 V
Backward	1.633 V

A. Flip flop pattern

In this method, flip flops were arranged to give particular pattern of output when the E-stop button is pressed. Though theoretically sound, clock jitters and overlaps renders this design unreliable based on testing results.

B. Direct Transmission

This is a much simpler technique, in which a 1 is transmitted if the E-stop button is pressed, and a 0 otherwise. The receiver then gives a 33% or 66% duty cycle signal to indicate a low or high level respectively. This is easily fed to the input of a properly sized (balanced) CMOS inverter to give a 0 if the E-stop button is pressed. This output is fed to the motors as supply voltage. As a result, whenever the E-stop is on, 0V is supplied to the motors, shutting them off. Otherwise, the output is Vdd and the motors can operate properly.

C. Antenna Design

The remote control has two wire antennas, one for each operating frequency. The length for each antenna is $\lambda/4$. Thus,
For 433 MHz, length= $1/(4*433*10^{-6}) = 9.18$ cm
For 315 MHz, length= $1/(4*315*10^{-6}) = 12.6$ cm

D. Remote Testing

Fig 3: Sky-Hawk radio controller

A Sky-Hawk 3-channel radio controller was ordered and subsequently dismantled in order to test its parts. The radio controller accepts eight 1.5 V AA batteries, making a total 12 V drop across the radio controller.

The left/right and forward/backward controls are used in the final complete controller design, as well as the chassis. The internal circuitry that came with the controller will be discarded in favor of the customized controller logic designed for the Minesweeper robot.

To test the left/right and forward/backward controls, a 12 V power source was hooked up to the entire radio controller to simulate the eight 1.5 V AA batteries that will be powering it, and a multimeter was used to measure the voltage drop across each control, which is 5.12 V.

A left/right or forward/backward control consists of a stick that can be pushed forward and backward or left and right, along with a variable voltage controller to the side.

A 5.12 V source was then hooked up to the V_{cc} and ground of the forward/backward control, and then a multimeter was used to measure the amount of voltage from the analog V_{out} pin as the stick was pushed all the way forward and backward.
It seems that there is a general difference of ~.5 V between the resting and forward positions' voltages at all the control settings, and a ~.6 V difference between resting and backward. Using this information, an Analog-to-Digital converter can be used to determine if the control is being pushed forward, backward, or resting, and send the corresponding signal to the controller logic. To facilitate this, the control will be left in the high power setting so as to output the most voltage so the A-to-D converter will have less trouble converting the signals.

IV. REMOTE CONTROL PROTOCOL

A. Design

The Radio Frequency Protocol was implemented to be a robust and effective method of conveying commands from the remote to the robot. This was done by sending data packets containing a summary of all guidance variables (direction of motion, turning info, speed info). This payload is couched in pre-determined start and end bytes. This is done to validate the reception of a valid packet and to eliminate effects of noise and possible interference by other signals operating at the same frequency as they will be discarded as void packets. The hardware for this communication is identical to the emergency stop setup, except that the chips communicate at 433 MHz

B. Sending a Packet

To optimize communication, a new packet is sent every time a variable value is updated to something different from its current value. This provides a much more elegant and safer technique than just mechanical thoughtless spitting of a packet at regular intervals of time. When this occurs, a flag value is set that calls a transmit function. This function synthesizes the packet from the payload and then transmits the data to the transmitter using the UDR(Universal Data Register) port.

C. Receiving a packet

The MCU receives packets through the digital DATA output of the transmitter from the UDR (Universal Data Register) input port. After a packet of desired length has been received, the interrupt is flagged. After this, an iterator is used to get all the bytes in the packet stored into an array. At this stage, validation checks are done by comparison of start and end bytes. Payload bytes are then read and used to update system variable values.

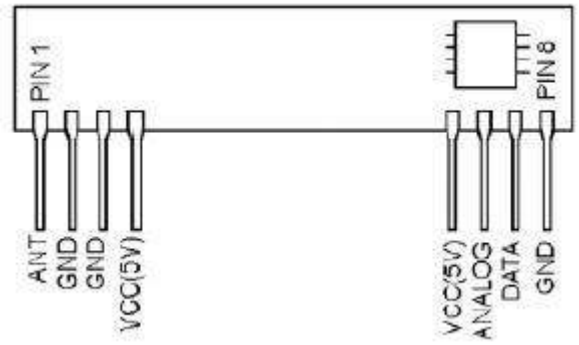

Fig 2: Pinout diagram for the RF receiver

D. Automated control

There are two possible setups in the case that a functioning navigation system is on-board. The remote control capability can be completely disregarded, and the remote thus used only for emergency stopping. However, for most applications it may be useful to have a switch on the remote control itself that can be used to disable the onboard system. When the automatic system is enabled, any RF packets received are disregarded and the variables are all set by decoding the packet received from the system computer instead, a process effectively identical to that of decoding an RF transmitted packet. When the automatic system is disabled, the remote uniquely decided the motion parameters.

V. MOTOR CONTROL

A. Overview

The motor control algorithm is implemented on a Mega128L chip in C. The implementation is for a 4 phase stepper with a cycle such as the following table:

TABLE IV
STEPPER MOTOR PHASES

STEP	A	B	$\overline{A}$	$\overline{B}$
1	+	+	–	–
2	–	+	+	–
3	–	–	+	+
4	+	–	–	+
5	+	+	–	–

This implementation is specifically designed for the Shinano Kenshi SS58D stepper motors provided with the ER1 test robot, but can be generalized for any stepper motor.

B. Implementation Details - Hardware

The design hierarchy is the following: The MCU outputs 4 signals, one corresponding to each of the signals in Table IV (Steps 1 and 5 are duplicate). Due to the nature of motor operation, there are inherent inductive spikes and noise that can damage the MCU. Thus, each motor input is isolated from the MCU using a photodiode pakage such as 4N35. This effectively isolates the MCU and the motor electrically.

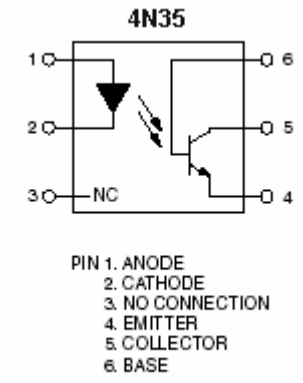

Fig 3: Optoisolator IC

As the motor can draw a fair bit of current, a second stage was added in the form of a power nMOS transistor, that can handle upto a maximum of 30W, 30V of V_{GS} and 17Amps of drain current. Such a transistor was placed to make the design extremely robust as the transistor can easily withstand the 12V

of V_{GS} and ≈1Amp that will be sourced from it and also withstand any spikes etc that can invariably occur. The driving circuit is shown in Figure 4, where the nMOS transistors illustrated are the power nMOS.

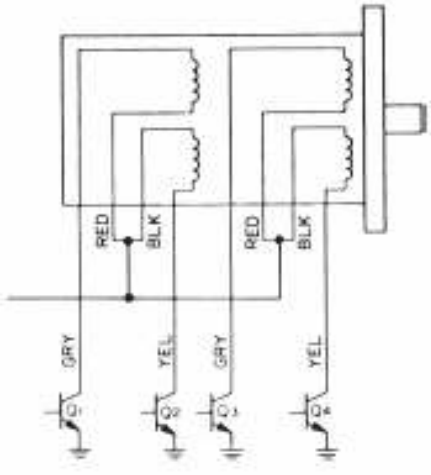

Fig 4: Motor Driver diagram

C. *Implementation Details – Software*

The core of the software to drive the stepper is a function that functions as a finite state machine between the four aforementioned phases, going forward step (1→2.. →5) for clockwise, and backward (5→4→..→1) for counter-clockwise. This function is called by the main subroutine based on the value of a software counter incremented by a timer interrupt function. The function is only called when the counter reaches a certain threshold, at which point it is also reset. The threshold is changed on the fly by inputs from the control mechanism on whether to increase or decrease velocity (Lower thresholds correspond to higher velocities as they are reached faster). The direction of the FSM is determined by a variable that maintains information about the current direction of motion (forward or backward). The core function has 2 FSMs, one for each motor. For turning purposes, one motor is turned off (The motor opposite in direction to the direction of the turn).

VI. Conclusion

The preceding sections delve into the implementation details of the control system. This system is to form part of the backbone of future Minesweeper robots of various configurations. For example, the main vehicle design is based on DC motors, that depend on a PWM output from the MCU. For this just the phase FSM function will be replaced by a PWM function. The ultimate aim would be to have a very portable firmware that works for several configurations and can be used for a particular setup by providing configuration variables values or setting them using jumpers in hardware. Looking to the immediate future, the aim would be to integrate and perform testing with the computer navigation system and DC motors so that it runs as a stand-alone robot.

Cornell MineSweeper: Power and Mine Detection

Hamzah Sikander, Michael Hsu, Mathew Meister, Timothy Russell

I. Introduction

THE power team spent the majority of last semester researching and designing the power distribution. However, since the design of the vehicle continues to change, so does the power requirements. This semester, the battery selection was finalized for the most probably final mechanical vehicle design.

Afterwards, the team switched focus onto landmine detection research. There are many proven and theoretical methods which were evaluated both in design feasibility and cost. While it would be great to somehow integrate as many into our vehicle as possible, methods such as canine-assisted detection and the use of biological systems are just not feasible for our goals. The goal was to research all proposed method and chose those that are most feasible for a moving vehicle to implement.

II. Batteries

A. Introduction

The objective is to choose a battery that has a suitable lifetime, weight, cost and actual runtime that is comfortable for research and commercial purposes. The structure of this section will revolve around defining the needs of our research / commercial and then the racing. This will followed by a detailed overview of our options, and then a market available product.

B. Requirements

Research would require small one hour session 'bursts' of power usage for their respective test runs on equipment. A single high power, long cycle life battery that is also light weight would be highly desirable. A fast charge time would also be desirable. Commercial use, though, would require a low maintenance, low cost, and high power solution with decent cycle life. The autonomous robot should be expected to make a run of almost 5 hours per day.

Racing would have similar requirements, but needs to have a higher discharge rate since it doesn't need to process the presence of mines, but rather just to accomplish the obstacle course as fast as possible. A run time of 50 minutes with a fast charge time would be desirable. Also it should be low cost, so we may afford a second for competition back up.

C. Overview of Battery Types

For cheap production and high durability purposes, standard lead acid batteries are the obvious choice. They are large and heavy but considerably cheaper and can easily meet the vehicle's power demands.

For high performance with a small form factor and mass, the Li-Ion or Li-Polymer batteries provide a near ideal solution. The original drawback was that each 12 volt battery can only supply up to 10-15 amps of current, and to meet our old peak current requirement of over 60 amps, at least four packs must be places in parallel. In addition, due to the delicacies of the batteries at high power outputs, protection circuits costing about $30-40 per battery are required. The estimated cost for four batteries including protection circuitry was $600. Due to changes in motor selection that dropped the current requirement to a maximum of 14 amps, Lithium Ion batteries are now an option, but cost is still a considerable issue.

Although it is several times the weight and twice the volume as the Lithium based batteries, NiMH batteries provide the best performing alternative. These batteries satisfy the spike current requirement and supply the next best energy density without requiring protection circuitry.

Because the end production vehicle will most likely be powered by lead acid batteries, the vehicle must be designed with at least 9000 cm^3 of dedicated battery space. Once the battery is chosen, recharging circuitry will be designed or purchase to allow for convenient and fast battery recharging. It is expected that the recharging circuit can be carried on-board so recharging becomes as simple as plugging the vehicle into an electrical source.

TABLE I A. BATTERY SPECIFICATIONS

Battery Type	Ni-Cd	NiMH	Lead-Acid	Li-ion/ Polymer
W/kg	150	150	180	1800
Wh/kg	45-80	60-120	30-50	150-190
Lifetime (months)	15	18-24	16	12-16
Cycle Life	1500-2000	300-800	500-800	300-500
Charge time (h)	1	2-4	8-16	1.5-3
Self Discharge/ month	20%	30%	5%	<10%
Operating Temperature (Celsius)	-40 to 60	-20 to 60	-20 to 60	-20 to 60
Maintenance	30 to 60 days	60 to 90 days	3 to 6 months	None

For our research and racing, the use of NiCd would be suitable. It provides a good lifetime, highest cycle life, fastest

charge time and very high discharge current. It is also light and cost effective.

D. Options

Both batteries are described in table I b., and both will apply a Nominal Voltage of 12 V with an maximum load of 235W.

For the Lead Acid Battery, the suggested battery available in the market is the TG-75 by Tempest Batteries. It comprises of a special chemistry that allows a small size (for Lead Acid), longer life and low cost. A Sub-Colloid Electrolyte makes the same specific gravity in every part of battery, thus preventing more effectively dropping out of activated substances. Special details on TG-75:

- Chemistry: Primarily Lead Acid; sub-colloid gel battery specifically designed for high discharge rate and long service life of 8-10 years. Sealed Construction: No electrolyte leakage from the terminals or the case; efficient operation in any orientation.
- High Energy Density: Large current discharge performance.
- Special Lead Calcium Alloy: Corrosion resistance and high recovery capacity.

TABLE I B.
BATTERY SPECS

Battery Type	TG-75	Custom NiCd
Rated Capacity	75Ah	20Ah
Watt-Hour	~900 Wh	240W
Expected Runtime	4.5 h	50 min.
Weight (Approx.)	52.90 lbs	12 lbs
Cost	$140	≈$350

Since our current consumption is 235 W (based on new motors donation), one should expect the total run time to be approximately 4.5 hours. This takes in account for the fact that the minesweeper's load will concentrate more on processing / detection, which requires far less power.

The second option is a custom NiCd Solution, which is just a conventional construction of taking NiCd batteries, and assembling them to our needs. This solution works better because it is flexible, and we are easily able to raise current and power if necessary. And although we will consume the battery withing 50 minutes, its recharge time is approximately 1 hour, whereas the TG-75 would require atleast 5 hours. Furthermore the NiCd is 12 lbs, which is easy to transport for our research purposes.

As a closing statement, I would like to commend that both options are economically viable, and both should be purchased for their respective purposes.

III. LANDMINE DETECTION

A. Introduction

Mine Detection Sensors are the most integral and difficult components for implementing an autonomous mine sweeping robot. Manual prodders who risk their lives would benefit first from better mine detection methods followed by having an autonomous/remote controlled robot. The methods we are researching are chemical methods, electromagnetic methods and a variety of seismic methods.

B. Chemical Methods

Chemical methods have the highest accuracy, precision and sensitivity among all detection methods. The search is particularly for the explosive package versus the non-volatile components of the mine, and although this method makes some mines immune due to terrain, weather and container design, it would be desirable to have such accuracy. The methods researched by CUMS were Fluorescent, Electrochemical, and NQR. Although NQR is does not exactly a chemical method, this was the most fitting category.

The basic principle relies upon waving the device above a suspected area, and as the fluorescent polymer films are exposed to air passing through, the explosive particles cling to the polymer causing a change in the brightness and wavelength of light emitted. The device is currently being tested by Nomadics Inc., who has accomplished, but is testing, a military grade, hand-held detection device. (See **figure 1**).

Strengths:

- Device can detect explosives from 10^{-15} g/ml, and future research will lower this threshold concentration.
- Easy to engineer to a hand held size.
- Since it is a vapor detection method, accuracy will not be stunted by physical features of a mine, which vary significantly.

Weaknesses:

- Is rendered useless against dry terrains, and due to its extremely high sensitivity, it will trigger many false alarms.
- Mines with their explosive package encased in metal will not be detected.
- Fluorescents may react with other unknown chemicals in the environment and trigger a false alarm.
- The technology is immature.

Figure 1: Nomadics Inc.'s fluorescent detector

One should conclude that the device is not ready for deployment for any type of mine detection since its probability of actually detecting a mine is far from perfect. Manual prodders would be preferred over a less than perfect device.

C. Acoustic Phase Array (APA)

An acoustic phased array (APA) consists of an array of emitters capable of sending out phased waves. We can adjust the region where constructive interference occurs by altering the phase shift of the waves each emitter sends out. The receiver then determines the presence of an object by the strength of reflected waves.

Although there has been research on using APAs underwater, research and experimentation on using APAs for landmine detection is lacking.

D. Electrical Impedance Tomography (EIT)

Electrical Impedance Tomography (EIT) is a method of imaging the conductivity of a medium by surface electrical measurements. Originally developed as a medical imaging technique, EIT is now being researched for the purpose of detecting buried landmines. By using electrical currents, EIT is able to measure the conductivity of the ground that is being probed and detect any discontinuity caused by buried objects.

Current EIT designs all contain 3 basic components:

- Electrode array (usually 8x8 array of spring loaded electrodes)
- Data acquisition system
- Data processing unit

Electrode array: The electrode array assembly is made of 2 Plexiglas plates (12.7mm thick) held together by 8 stainless steel support rods (9.52mm diameter). The plates are 110x110cm and are held 15cm apart by the rods. The assembly supports the metal enclosure containing the data acquisition electronics and holds the individual electrodes in place. The distance between two electrodes, also known as the electrode spacing (ES), is 14cm.

It was determined experimentally that when a force of about 6.7N (1.5lb) is applied over that type of electrode a reliable electrical contact is usually established with the soil.

Data acquisition system: Incorporates the electronics and firmware required for the electrical stimulation of the electrodes and the recording of the resulting potentials. The EIT instrument is a high precision impedance meter. It uses four electrodes to perform a transfer impedance measurement. Two electrodes are used to inject a current into in the medium and two others to measure the potential difference developed on the medium surface.

EIT data acquisition electronics is physically partitioned into three main subsystems: switching logic - selects the stimulating and recording electrode configurations signal preprocessing circuitry – applies a gain and filters the incoming signals control and measurement subsystem – generates all necessary signals for the system to work. The typical stimulation current and frequency is on the order of 1mA and 1kHz.

The data processing unit: is the software application that processes the raw measurements using a mine detection algorithm based on a matched filter approach.

The detector response is pre-calculated for a replica of the size and shape of the object of interest—for a number of grid locations underneath the detector. A correlation is then performed between the detector response for the replica and the actual detector response obtained from the measurements, for all the replica positions considered. The position that yields the largest correlation value is identified as the most likely position for the mine.

Data and estimations are based of the work of Philip Church and John McFee with their prototype EIT detector aimed at antitank landmine detection.

As a general rule, reliable detections are obtainable down to a range of 1 to 1.5 ES for objects with a size on the order of 2 ES. This means a 28cm diameter antitank mine results in a detection range of about 15-20cm in depth.

The detection of targets down to a depth of 17cm has been successful in all cases. The matched filter approach of processing data is very efficient at reducing the false alarms caused by objects of different sizes.

Data acquisition time is on the order of 1 second for a complete scan. Data processing based on a matched filter implemented through matrix operations takes a few seconds in Matlab but can be improved through the use of dedicated processors.

EIT Strengths:

- Disturbance in soil electrical conductivity does not depend on whether the mine is metallic or not.
- Good performance in wet areas due to conductivity.
- Relatively low cost.

EIT Weaknesses:

- Electrode-soil contact may be difficult in certain terrains and is potentially dangerous due to proximity to mines during contact.
- Good measurements depend on the medium being electrically conductive making dry sand or rock covered surfaces problematic.
- Multiple layers of soil having different conductivities.

To better understand the performance of an EIT detector, field trials in different environments are required. This would allow performance to be documented in terms of receiver operating characteristic (ROC) curves.

The next step of EIT detectors is to design & evaluate better deployment. Conceptual deployment platforms include, for example, remote-controlled rovers equipped with electrode embedded in tracks or flexible mats with embedded electrodes to be dragged along the surface.

E. Electro-Magnetic Induction

EMI in short, defines a metal detector. With an excellent sensitivity to any metallic components in a mine, it is usually the first step for finding a suspicious object for manual prodders. Unfortunately, there are far too many false alarms, which is expected from naturally found objects and exploded mines' shrapnel.

The probability problem is evident in most detection methods, but what can be reduced is the overall interrogation time by supplying more information. Mine detectors, sadly even after many years of inventing it, are still very crude. It simply does nothing except tell us a metal object exists.

EMI sensor array:

The topic of research for sensors next semester should revolve around describing the shape or size/mass of the metallic object. The idea would be similar to EIT, and instead of having electric probes, one would have smaller versions of metal detectors; an array of small metal detectors. It should be understood that there are obvious problems, such as interference due to external sources and side by side metal detectors, noise, displaying the object etc.

To conclude, EMI sensor arrays look promising as a cheap solution that could reduce interrogation time and the fatal risks of manual prodding.

F. Infrared/Hyperspectral

Currently, there are three main detection methods using infrared (IR) sensors to detect landmines – passive thermal detection, active thermal detection, and passive detection of nonthermal surface phenomena.

Passive Thermal Detection

The basis behind this method for landmine detection lies in the physical characteristics of the soil itself. When the sun heats up the ground, the soil emits a thermal radiation detectable by a thermal IR sensor. What allows someone to know if a landmine were present using this method would be changes in the thermal readings coming from the sensors. This comes from the fact that the mine would be a better thermal insulator than the soil, therefore able to absorb more of the radiant energy from the sun without as much radiation. Currently, most thermal detection methods employ a "snapshot" method which take multiple thermal images of a region of interest are over a certain amount of time. However, this method does have its setbacks. While the general idea behind determining the location of a mine seems simple enough, the actual readings that the sensors provide can be highly variable, depending on factors such as time of day, prior solar illumination, wind speed, ground cover, and soil contents. All of these are natural factors which can range widely between different areas, and even within the same region itself. Light reflections causing surface clutter as well as inhomogeneous soil can also cause issues in the gathering of data. These inconsistencies can often be large enough to seem like landmines, causing a large number of false-positives. Foliage can also interfere with the readings, as it can mask the temperature of the soil underneath.

Active Thermal Detection

This method differs from passive thermal detection in that it does not rely on solar heating which is very susceptible to environmental conditions. Active methods replace the sun with concentrated optical or high-power microwave sources. Because the properties of soil lend itself to be easily heated by external sources, and most mines are made from either plastic or metallic substances, it is easier to see the differences in thermal radiation. Additionally, the mines can produce standing wave ratios with the reflected magnetic fields from the microwaves. Unfortunately, as of now, this method requires prolonged exposure before accurate readings can be ascertained.

Passive Detection of Nonthermal Surface Phenomena

Because soil is made up of various particles of different sizes, one can also use how the average particle size changes to determine where a landmine is. During the burial of a landmine, the smaller particles are brought to the surface. This aspect can be taken advantage of through hyperspectral sensors. However, vegetation has proven to be a significant setback in this method. Rainfall can also have an adverse effect on how effective this method is.

An image of what some of the imaging solutions look like when detecting:

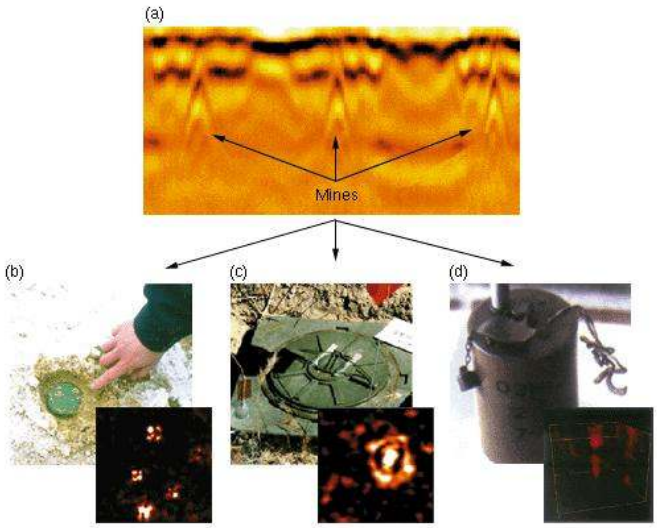

Figure 2: Infrared/hyperspectral imaging of lanmines [4]

G. Acoustic-To-Seismic

The idea behind this method of landmine detection is to use sound to penetrate the ground and excite resonances in buried objects. Sound produced in the air can typically reach down to about .5 meters into the ground due to the porous nature of most topsoil, creating acoustic vibrations that are sensitive to buried landmines. The sound source can be as simple as off-the-shelf speakers, and readily available Doppler vibrometers can be used to detect the added vibrations from the landmine reflections. This method of landmine detection takes advantage of three main facts that have not been exploited to the full potential before. The first is that landmines are man-made, and are therefore much more compliant than soil, creating high-vibration contrast between it and the soil. The second fact being exploited is that landmines are nonporous objects, which helps to further create a contrast between it and the soil. Finally, the interface between landmines and the soils around them has been shown to be nonlinear, and is therefore not continuous under vibrations. Unfortunately, this method does have some serious drawbacks. The ideal operating conditions for this methodology is in dry, sandy soil areas. Any conditions that don't fit this environment can seriously hinder the depth to which the signal can effectively reach. This makes realistic depths to be less than 30 cm. Also, other random objects in the ground, such as buried soda cans, will also trigger a similar response to a landmine, leading to a fair number of false-positives. Testing has also shown hard, frozen ground to be a serious problem as well.

IV. Conclusion

The teams switched focus this semester from power distribution to landmine detection.

Next semester, the team must begin implementation of the landmine detection scheme. In addition, the power distribution design from the first semester must be made a reality and integrated into the vehicle.

Table 2
Power and Landmine Detection Team Goal (Fall 2007)

September	• Purchase batteries • Determine and purchase recharging solution • Finalize power distribution design with updates for the final mechanical design • Decide on the appropriate combination of landmine sensors
October	• Order PCB boards for the power distribution • Purchase landmine sensors • Work with sensors team on sonar integration
November	• Test and implement landmine sensors • Implement power distribution on the vehicle • Test the distribution system for all loads and voltage rails using the battery
December	• Make all final adjustments to power • Continue testing landmine sensors • Join sensors team on integration

V. References

[1] "Alternatives for Landmine Detection." RAND. 15 Apr. 2007 <http://www.rand.org/pubs/monograph_reports/MR1608/>.

[2] Church, Philip, Philip Wort, Stephane Gagnon, and John McFee. "Performance Assessment of an Electrical Impedance Tomography Detector for Mine-Like Objects." Difference Defense. 15 Apr. 2007 <http://www.dres.dnd.ca/reports/English/SPIE2001-EIT-final.pdf>.

[3] "Electrical Impedance Tomographic Imaging of Buried Landmines." IEEE Xplore. Cornell University.

[4] "Making Landmine Detection and Removal Practical." Landmarc. 07 Apr. 2007 <http://www.llnl.gov/str/Azevedo.html>.

Cornell MineSweeper: Sensors

Nana Wu, Jehhal Liu, Chin-Hung Chen, Timothy Russell

***Abstract* — The aim of Cornell University's Minesweeper project is to create a cost effective autonomous robot which will detect landmines more accurately than current de-mining devices. One of the Minesweeper's features is an obstacle detection and navigation system to minimize the need for constant human supervision. The objective of the sensors team is to develop such an avoidance system by using strategically placed sonar sensors to measure the distance of the vehicle from any object in its path. The vehicle can then plan how to maneuver itself around the obstacle accordingly. In addition to sonar, the sensors team is also responsible for the integration of a Global Positioning System and Inertial Measurement Unit for determining the positioning and acceleration of the vehicle. This report describes the key developments which the sensors team has made this semester along with a plan for future action.**

I. INTRODUCTION

Throughout the semester, the sensors team has been working with sonar obstacle detection units. Research and testing of the units has been performed. The optimal configuration with respect to reliability and efficiency has been determined for use in an automated vehicle.

The GPS and IMU units both have been integrated and tested in a linux environment. Engineering trade-offs must be considered before integration onto the vehicle.

II. SONAR RESEARCH

Preliminary research began last semester. Initially, devices were researched which could be used to detect any obstacle around the vehicle. The range of such a device needed to be between 0.22 meters (0.73 ft) to 10 meters (32.8 ft), so that the vehicle can navigate around the obstacle. Six potential productes were found which matched specifications. Ultimately, the MaxBotix EZ-1 sonar unit was chosen because it was inexpensive, reliable, and easy to handle. The sensor chosen has the following properties:

- 2.5V to 5.0V operation
- 2mA current draw
- Serial data output
- Analog voltage output (voltage ~ distance)
- Range of 6 inches to 200 inches (~15cm to 500cm)
- Continuous measurements (can be triggered externally)
- Fast measurements (max. of 50ms per reading)
- $25 per unit

The MaxBotix EZ-1 Sonar Range Finder is very small and therefore will not take up much space on the vehicle. The dimensions of the sensor are shown in Figure 1 below:

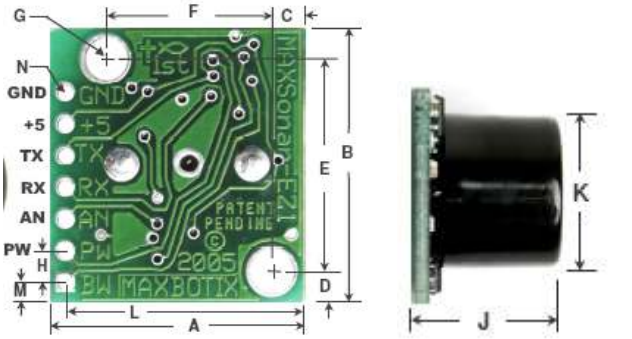

A	0.785"	19.9 mm
B	0.870"	22.1 mm
C	0.100"	2.54 mm
D	0.100"	2.54 mm
E	0.670"	17.0 mm
F	0.510"	12.6 mm
G	0.124" dia.	3.1 mm dia.

H	0.100"	2.54 mm
J	0.645"	16.4 mm
K	0.610"	15.5 mm
L	0.735"	18.7 mm
M	0.065"	1.7 mm
N	0.038" dia.	1.0 mm dia.
weight, 4.3 grams		

Figure 1. The above diagram shows the dimensions of the sensor. Since the unit is very small, putting many sensors onto the vehicle will be simple and will not cause any cluttering.

III. TESTING OF THE SONAR PROTOTYPE

After the prototype arrived, it was tested by following the possible patterns of the sonar sensor. The detailed testing of the sonar sensor was carried out by observing the precision of the measured distance versus the actual distance from an object. From the test results, the data specifications provided by the manufacturer were adjusted, since the actual range of vision had some discrepancies. It was decided to use the sensors to detect obstacles at a range their peak accuracy within a 30 by 100 inch area, 50 inches in front of the sensor, as seen in Figure 2. The measurements appearing in Table 1 show the maximum lateral distance from the sensor for which the data output still gives a continuously accurate reading. All the data collected in this experiment was taken using the analog output of the unit, which outputs ~9.8mV per inch distance between the sensor and the object being detected.

Table 1
Data collected from prototype testing (inches)

Distance from sensor	Distance Left of the axis	Distance from sensor	Distance Right of the axis
25.5	-48	46	11.5
32	-62	60	15.5
46	-19	67	16
66.5	-27	79	25.25
76	-39	88	25.5
89.5	-40	97	30
92.5	-36	99	23
110	-40	117	30
117	-38	119	22.5
117.5	-47	125	18
138	-32	137	15.5
139	-35.5	144	20
157	-25	149	13.5
170	-11	161	0
162	-20		

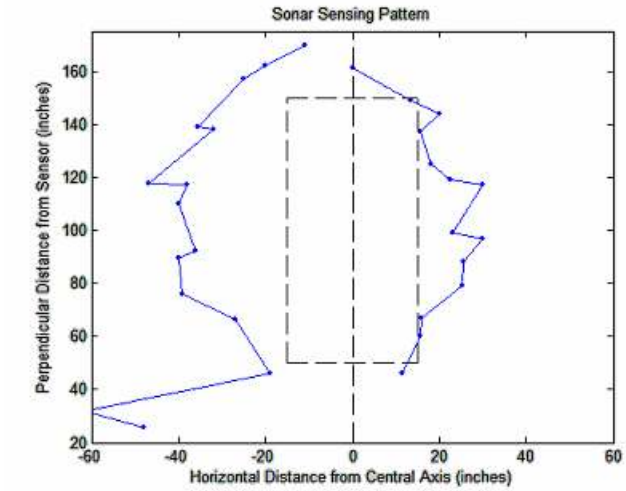

Figure 2. Sonar pattern plotted from the data collected, each point representing the distance from the central axis. The vision of the sonar starts narrow and is the widest at around 110 inches from the sensor. As distance increases the width of the vision tapers off. Sensor is located at the origin of the graph.

IV. Layout of the Sonar Sensors

Taking the limitations of the sonar into consideration, various possible layout schemes were considered for the placement of the sensors on the Minesweeper vehicle.

The original design for the layout was laid out so that the front of the vehicle had the widest range of vision. Placing the sensors solely perpendicular to the sides of the vehicle would leave large blind spots in the corners, which could cause problems when the vehicle makes turns. Therefore, the preliminary design was to place three sensors on the front of the vehicle, one on each side facing out to the right and left, and two on the top which are directed out by 45 degrees to point towards the direction that the robot was turning. The design can be seen in Figure 3 below. This design was later altered to place more sensors on the sides, to ensure that the vehicle has optimal vision around the perimeter in order to avoid any structural damage.

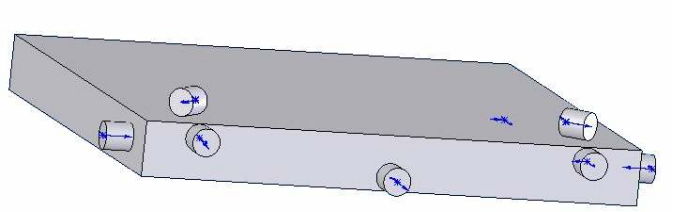

Figure 3. The original idea for the placement of the sensors around the vehicle. Three sensors were placed in front to ensure avoidance of all obstacles directly ahead. Sensors on top were added to catch any obstacles while turning.

The final configuration minimizes the blind spot of the vehicle and provides the widest and most useful field of detection. The sensors on the front of the vehicle were positioned such that two sensors were placed higher on the sides than the middle sensor which was placed closer to the ground. Same layout applies to the two sides of the robot but shifted more toward the front edge of the vehicle. Figure 4 shows the layout from two different views.

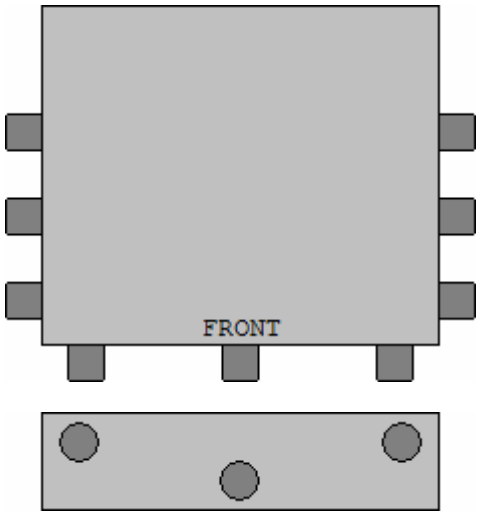

Figure 4. The sensors will be arranged around the vehicle as described above. The top figure shows a birds-eye view of the vehicle, showing how the sensors will be arranged around the perimeter. The bottom figure shows a head-on view, showing that the middle sensor on each side will be set lower than the other two sensors.

Another limitation that was taken into consideration is the fact that these sensors use sound waves. These waves could potentially interfere when two or more units are in use simultaneously. For instance, one sensor could pick up a sound wave that was emitted from a different sensor at an earlier time, thus changing the outcome of the distance reading. Also, when two sensors emit their sound waves at the same time, the two waves could return completely out of phase, in which case the waves would be cancelled out, causing the sensor to miss the obstacle completely. In order to avoid this problem, the sensors will need to be carefully operated, taking into account any detrimental physical effects that could occur during usage. One

possibility is to ensure that sensors used simultaneously within a 50ms span be pointed in completely different directions.

V. Serial Port Connection

Initially, simultaneous control of multiple sensors using a RS-232 serial port was attempted. After soldering one sensor onto the port, range detection was successfully performed with a single sonar sensor. However, the difficulty arose when several sensors were connected to the same serial port. The unit could not be controlled and the data could not be read using just one port. Since each of the nine pins on a RS-232 port has a specific function, the sonar units cannot be individually connected to independent pins/ . At first, we thought only a few of the nine pins were needed to serve as power supply, ground, input signal and output signal. Though power, ground and input pins could be implemented easily for multiple sensors, collecting and converting the obtained output readings from our sensors to a serial format was unsuccessful. Therefore, it was concluded that in order for all nine of our proposed sensors to work at the same time, nine serial ports would be necessary. Since this option is not feasible, other methods for simultaneous multiple sensor operation was considered.

VI. Linking Multiple Units in Series

The next step was to try linking multiple units in series, based on a diagram given on the manufacturer's website. Using one resistor, and one diode per unit, the manufacturer suggested that it was possible to obtain data from multiple sensors by measuring the pulse width of their output. After linking two units together, it was found that the detection of the pulse widths was impractical and perhaps too difficult to be performed correctly and accurately. Furthermore, it was later found out that the manufacturer had stopped recommending this layout because noise affected the output greatly. Because of the multiple I/O ports available on a microcontroller, it is an ideal solution for collecting data from the sonars and then sending them serially to the computer for processing. The microcontroller can send out commands to each sonar to take a reading. When the microcontroller has received all measurements, they can be strung together and separated by a character. A packet is then sent serially to the computer while the next set of measurements is taken. The specifics of such an operation will be determined next semester.

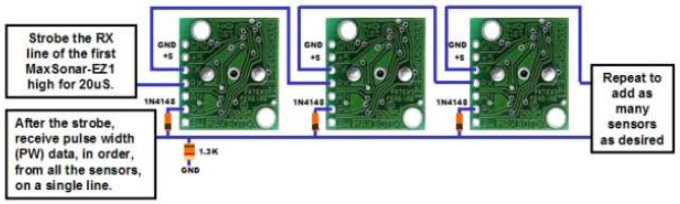

Figure 5. The layout suggested by the manufacturer. One diode is needed for each sensor and one resistor for the entire set up. PW is the output collected as the pulse width of the output represents the range detected.

VII. Sonar Enclosure

An enclosure is necessary for the sensors to properly operate outdoors. Since the sensor itself is designed to be used in an indoor environment, a protective covering is necessary. While most of the enclosure could be made of anything that satisfies the conditions, the front of the enclosure must be permeable to sonar and not affect the readings of the sensors. After trying out various materials, including glass, wire mesh, plastic, elastic material and fabric, abrasive foam was decided upon. This material would be able to protect the sensor while still being permeable to sound so that the sensor could still make accurate readings.

VIII. Sonar Future Objectives

After testing various methods of operation, the original design was decided against. A microcontroller will be used to collect the output of the sensors and relay the data to the main computer.

After successful communication between the computer and the sensors is obtained, cooperation with the mechanical team is necessary to construct the final layout of the nine sensors distributed throughout the vehicle. After mounting the sensors onto the vehicle, the final design can be tested to see if the vehicle can maneuver while avoiding any obstacles in its path.

Upon the completion of the sonar system, research and implementation of short range sensors will be considered. These are used to detect any objects within six inches or less of the vehicle. They are essential because the sonar sensors cannot operate reliably in such a short range. These short range sensors will be used as a backup system to ensure that no objects come close enough to the vehicle to damage the unit.

IX. GPS Implementation

The GPS purchased is the uBlox AEK-4T timing kit. It includes a processing unit, antennae, and USB connection. All power is derived from the USB port. The GPS unit includes a Windows driver with accompanying software. However, the on-board computer on the vehicle is specified to be operating in a Linux environment most likely with a Debian flavour. Thus, the goal for GPS implementation is to find a solution for integrating the GPS unit into a Linux environment and test its accuracy.

Fortunately, typical GPS unit operate by communication using National Marine Electronics Association standard sentences. These sentences are begun by a word which determines how the remainder of the packet should be interpreted. Because the unit uses the NMEA standard, a daemon can simply run on the computer interpreting this stream of sentences.

A daemon named GPSD is capable of interpreting all NMEA sentences. This open-source solution operating on the Linux kernel permits easy parsing of the sentences. A simple perl script was written to connect to gpsd and parse the output for latitudinal, longitudinal, altitude, and speed information. This information can be passed onto other programs and scripts running on the vehicle computer.

To view the GPS output, a program called XGPS was run which displays satellite positions and all relevant data according to the GPSD parsed NMEA sentences.

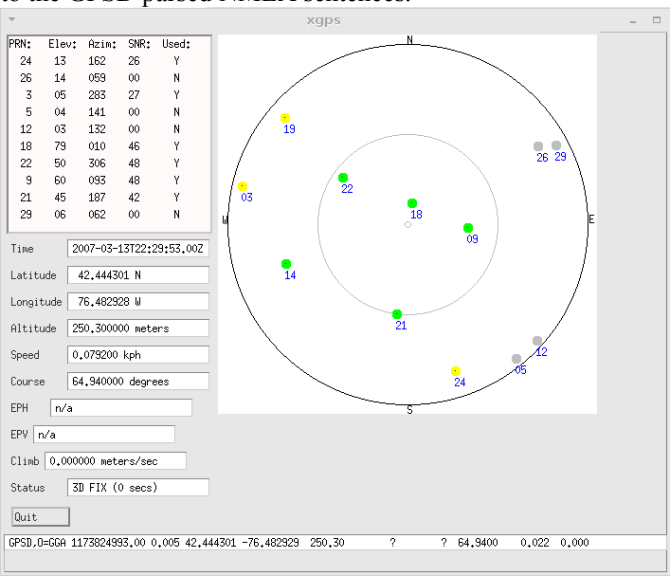

Figure 1: XGPS output using the uBlox GPS unit

To test the unit, a perl script was run which outputs the longitudinal and latitudinal position every second. The GPS unit was moved a set distance of 10 meters due south. This is movement in the latitudinal direction.

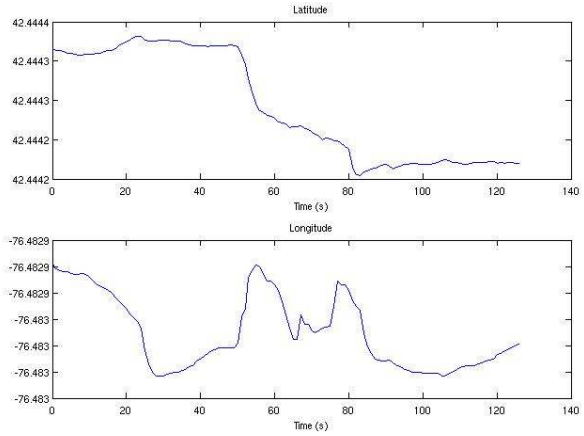

The plotted results show noise in the longitudinal direction but a convincing change in latitude. This change is about 0.0001 degree change in latitude. Taking into account the latitude and curvature of the earth, this difference corresponds to a change in distance of 11.108 meters. Thus, the GPS is relatively accurate. Over a range of 10 tests, the average difference in distance was 15.3%. This corresponds to reasonable results. This is too high for any reliable speed calculations but appropriate for relative positioning.

X. IMU Implementation

An inertial measurement unit is typically used to detect altitude, location, and motion. These units are typically composed of accelerometers, angular rate sensors, and a processing unit to make calculations as a result of the sensor outputs. Change from initial positions is calculated from the current acceleration and rate of change in altitude.

The unit received for testing is the Kionix KXM52-DEV-V1. It is in actuality just an accerometer board and not a true IMU because it lacks both the gyroscopes and processing unit. As a result, it is not just a plug and play solution.

The unit is again packaged with just Windows software and a Linux solution must be created. The on-board MCU performs the analog to digital conversion and is programmed to respond to commands on an RS232 serial port. The byte commands are as follows:

Code	*Description*
X	Send X acceleration
Y	Send Y acceleration
Z	Send Z acceleration
A	Send X,Y, and Z Accelerations
T	Send T (Echo Command)

Although, a Linux driver is unavailable, raw serial communication can be used. This again just requires a script to communicate with the on-board microcontroller.

The steps required to obtain an acceleration in units of g are:

1. Configure serial port (Baud rate, parity settings, data rate, etc.)
2. Open the serial port and send the echo command to ensure the microcontroller is on and operational
3. Send the 'A' command
4. Receive X, then Y, then Z accelerations in serial
5. Divide all three by the analog to digital ratio of 1241.2121
6. Subtract the offset of the accelerometer of 1.650
7. Divide by the sensitivity of the accelerometers

This process is written in a simple perl script.

The most difficult portion of using the board is that the velocity and distances must be calculated. Current velocity can be predicted from a reference velocity plus the acceleration times time. Knowing the time between acceleration values, the change in velocity can easily be calculated. This is added to the previous period's velocity to determine the current. The distance travelled then can be estimated using the average of the current calculated velocity and the previously calculated velocity multiplied by the change in time between the two values.

Angle of tilt can also be roughly estimated by taking the arcsin on the Z axis.

Noise on acceleration propogates through all of the calculations and is additive from the original known reference velocity. This is one area where the GPS can come in handy. Close to a known velocity such as a stopped position, the accelerometer based velocity and position will be accurate and can be used to calibrate the GPS. Later as noise propogates through the system, the GPS can be used to check the sanity of these values.

The accelerometer board is a useful tool for the autonomous vehicle. If possible however, a full IMU solution is recommended for accuracy and to reduce the processing strain on the on-board computer. The current solution will suffice if necessary and is easily integrated into a Linux environment.

XI. Conclusion

During the spring of 2007, the sensors team has mainly worked on finding a practical way to communicate between the sensor and the main computer of the vehicle. Although many difficulties and set backs were realized, the team remains on the right track to completing the implementation of the sonar sensors and begin designing the short-range sensors system next semester.

Table 2
Sensors Team Goal (Fall 2007)

September	• Take in depth look at our microcontroller • Learn any necessary coding skills • Write code for data collection • Research on short range sensors • Finish IMU implementation
October	• Hardware connection of sensors and microcontroller • Testing of the implementation • Design the implementation short range sensors • Integrate IMU and GPS with the on-board computer
November	• Physical integration of sonar sensors onto the chassis • Field testing of sonar sensors • Solidify and finalize the design of short range sensors system
December	• Make any revision of sonar sensors • Purchase necessary components • Realize goals for Spring 2008

Cornell MineSweeper: Drivetrain Design and Analysis

Vikas Reddy, ve23@cornell.edu

Abstract- This paper covers the design process for Cornell MineSweeper's Robot drivetrain. Two concepts were designed and analyzed and a recommendation is made. The recommended in-wheel motor design will be fabricated over Summer 2007.

I. Introduction

The drivetrain encompasses all mechanical systems that propel the robot and this includes the motors, the wheels, the transmission and the suspension. The suspension is discussed in detail in the Suspension report and this report will only focus on the former three components.

TABLE I
DRIVETRAIN SPECIFICATIONS

Item	Specs
Maximum Speed	2.23 ms^{-1}
Crusing Speed	1.5 ms^{-1}
Drive Mode	All Wheel Drive
Steering	Skid-Steer
Power	Electrical/Chemical (Battery only)
Transmission	Direct/ In-line
Wheel size	6" dia. / 0.15m dia.

A. Specifications

The current robot is designed to handle both, the rigors of a minefield and also that of the Intelligent Ground Vehicle Competition and the specifications are shown in Table 1.

The specifications for the speed and power are constrained by IGVC's rules while the remaining specs were chosen after a thorough literary research and analysis of all terrain robots such as the NOMAD and the Mars Exploration Rover.

B. Motor Selection

Since the power source was limited to a battery, the obvious choice for propulsion was an electric motor. And since the robot was to be a low power consumer, the Permanent Magnet DC motor was the best choice. Also, since DC motors are high speed, low torque devices, it was evident that a gear box would be critical. So, to simplify our task, it was decided to purchase a PMDC gear motor. More specifics about the motor shall be discussed under the sections Drivetrain v1.0 and Drivetrain v2.0.

C. Transmission

The first stage in the transmission is the gearhead which increases the motor torque. The second stage is the linkage between the gearhead shaft and the wheel. Since the motor and gearbox are high precision devices, it is critical that the shaft is isolated from all shock and hence it cannot be directly in contact with the wheel. Two options were considered – use a universal constant-velocity joint or use a shaft coupling. The details are again discussed under the two design versions.

D. 'Wheel' Selection

After considerable debate regarding the use of wheels vs. legs vs. whegs vs. tracks, wheels were chosen as the simplest and most effective way of propelling the robot largely due to the fact the landmines are pressure sensitive devices and legs/whegs exert high ground pressure. Tracks would have been a better alternative with regards to ground pressure, but the amount of ground resistance is a lot higher with tracks and hence, makes them highly inefficient.

Also, wheels could be designed such that they exert lower ground pressure by either choosing a large number of wheels or by making the wheels wider or both.

After some literary research, it was established that there were a lot of unknown parameters in our problem statement and hence, an accurate determination of the number of wheels could not be made. The entire process described by *Apostolopoulos et al* was studied and the sinkage, soil thrust and ground resistance parameters were plotted as in Figures 1,2 and 3.

From the graphs it is evident that a larger wheel has lower overall resistance and hence is more efficient. However, a larger wheel also means a higher torque requirement on the drivetrain and thus a tradeoff needs to be achieved. After tweaking the diameters around, it was decided to use 6" wheels.

However, no conclusive results were obtained regarding the number of wheels and so, it was decided to follow a tried and tested approach and based on the MER it was decided to use 6 wheels, since it reduces ground pressure and also provides more driving torque in situations of bad ground contact where one or more wheels might lose contact with the irregular terrain.

II. Drivetrain v1.0

The first drivetrain design was completed by mid-March and incorporated six wheels sporting an all-wheel drive powered by two PMDC motors. This design was inspired by the Journey Bot and its specifications are described in the report's Semester Overview section.

This robot weighed around 50kgs due to the use of a Lead acid battery which alone weighed 25kgs. The power requirements to propel this robot were high at 650 W using a drivetrain efficiency of 70%, coefficient of rolling friction of 0.25 (sand), a incline of 20% and a velocity of 2 ms^{-1}. These requirements are that of the worse case scenario and the calculations were performed using equation 1. Air resistance was ignored since the robot is only traveling at 5 mph, a speed at which drag force is negligible.

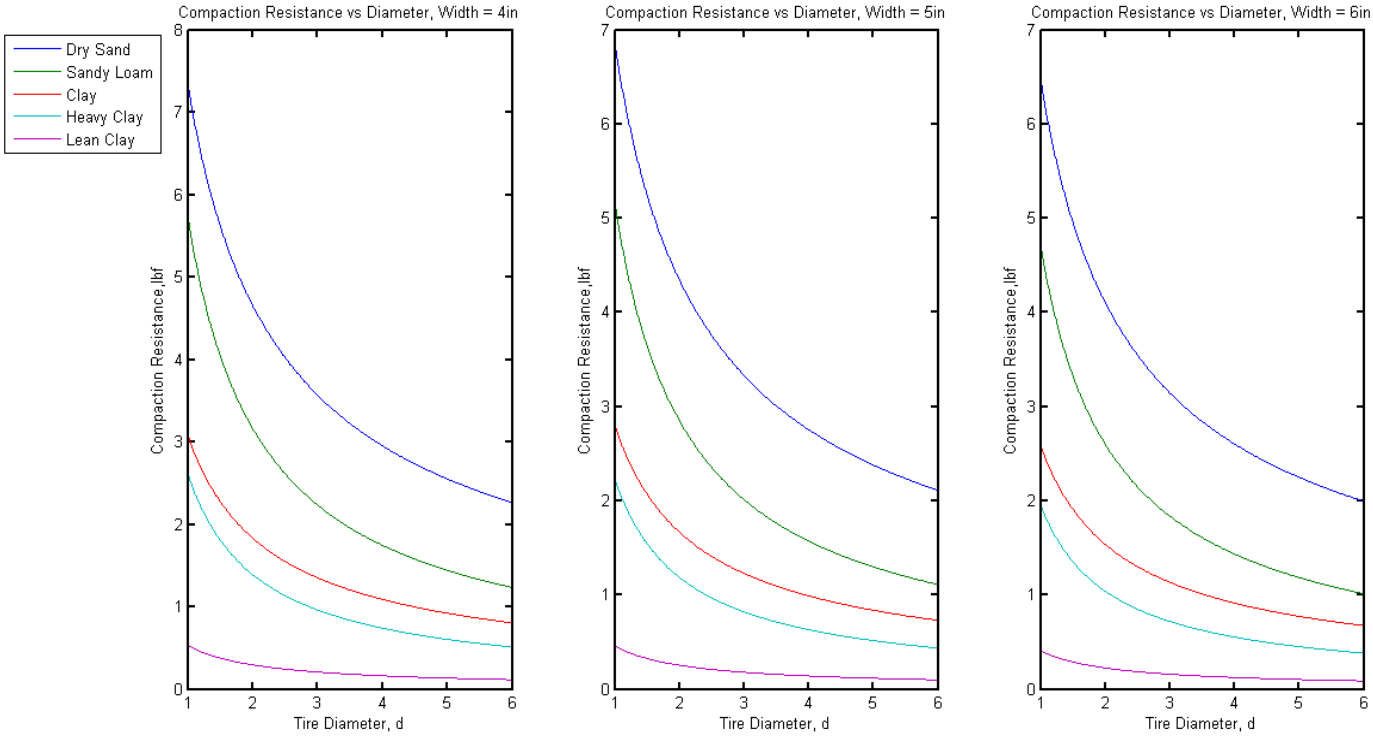

Figure 1: Soil Compaction Resistance vs. Wheel diameter.

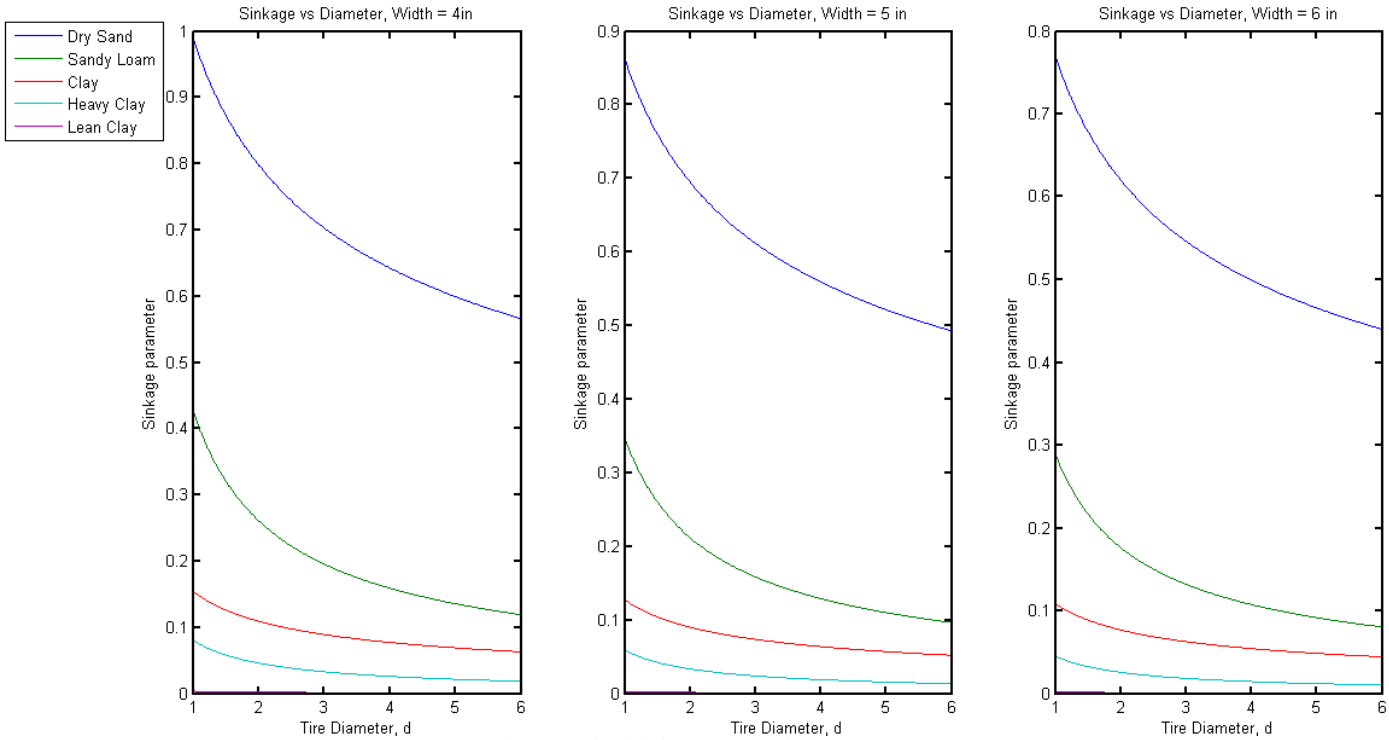

Figure 2: Wheel sinkage vs. Wheel Diameter.

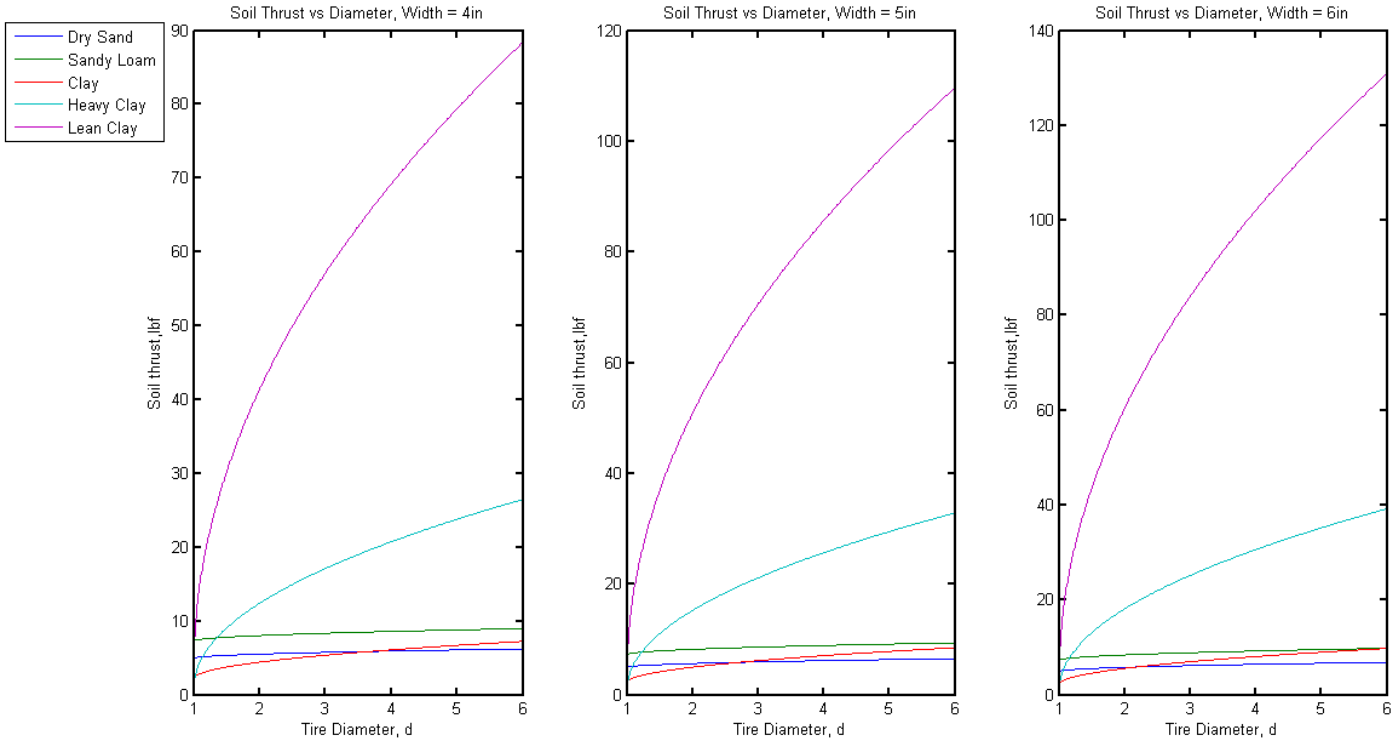

Figure 3: Soil Thrust vs. Wheel Diameter

$$P = \frac{(P_{rolling} + P_{gravity} + P_{accelerate})}{\eta}$$

$$P = \frac{m(a + g\sin(\theta) + \mu_r g\cos(\theta)) \times v}{\eta}$$

(1)

Due to such a high power requirement, two Moog Silencer Series motors with power ratings of 300W each were chosen and the torque was amplified via a timing belt-drive transmission using parallel pulleys and then linking the pulley shafts to the wheel via a CV joint. The system is shown in Figure 4.

The wheels are 5.5" GRP Tractor series bought from Tower Hobbies. They are 3.3" wide and have good ground traction.

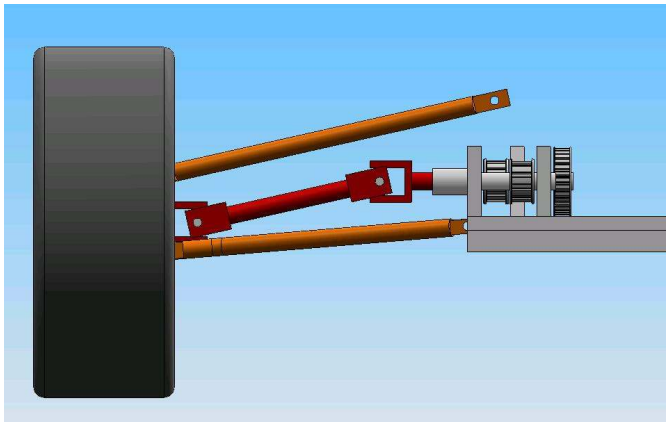

Figure 4: Timing belt-pulley, CV joint and Wheel linkage.

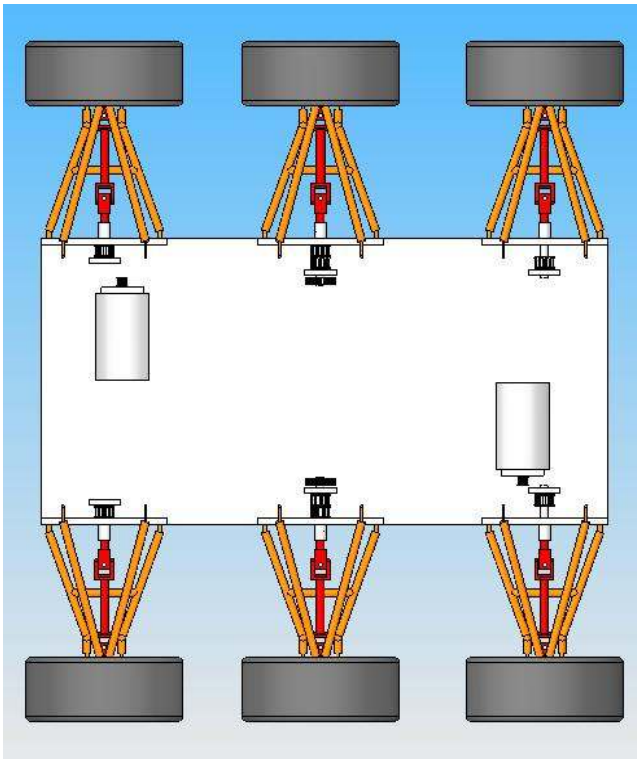

Figure 5: Drivetrain v1.0. Notice how the motor connects to the central wheel directly and how the outer two wheels are powered from the central wheel.

A. *Pros*

- Robust with high tolerance for misalignment amongst shafts.
- Inbuilt damping due to the use of timing belts
- Two motors simplify control system
- System is self-regulating with respect to torque. If one wheel loses contact with the ground, the other wheels have a higher stall torque.

B. *Cons*

- CV joints and belt-pulleys are highly inefficient.
- Too many moving parts and linkages in series. If one timing belt fails, atleast two wheels lose power.
- Motors weigh 5kg each, with the CV joints and pulleys weighing an additional 1 kg for each wheel.

III. DRIVETRAIN V2.0

The team received a donation of 6 Faulhaber motors with gearheads from CU Snake Arm. The motors were Faulhaber 2342CR 24V with 23/1 gearheads having 43:1 (four) and 66:1 (two) reduction ratios as shown in Appendix A.. These motors have a high power/torque density and cost an average of $200 a piece. They provide continuous working torque of 0.7 N-m and 1.0 N-m respectively at 19W each and they weigh 0.170 kg each.

Since these better motors were available immediately, the team redesigned the drive train to incorporate the new motors and strived to achieve a much lighter and efficient drivetrain.

Equation 1 was used to tweak the robot's velocity and with the available 114W of power, the robot weighing 25 kgs can travel at 1m/s on a sand incline of 20% accelerating at $0.2 m/s^2$. Under nominal conditions, the robot has a speed of 2.1 m/s.

The new drivetrain incorporates an innovative in-wheel motor design where each wheel is a fully contained modular propulsion unit requiring only power and control signals from the main body.

Since all the motors don't have the same torque, the two motors with the higher torque will be placed in the middle two wheels since there is a higher likelihood that these two wheels will always remain in contact with the ground when compared against the leading and trailing wheel.

The wheels itself are custom designed with two 6" Al-6061 discs of ¼" thickness with sheet metal flats serving as tires as shown in Figure 3. This design exerts lower ground pressure since the ground contact is always over a wide flat area and also, these wheels have a lower moment of inertia compared to conventional tires such the of the same diameter.

Since the motor is in the wheel, it is more susceptible to shock and thus, the shaft needs to be isolated.

A shaft coupling was considering initially, but they are expensive, bulky and heavy. Instead, a nylon tube with ¼" ID and ½" OD will be used to connect the wheel shaft to the motor. The effectiveness of this design can only be established after thorough testing.

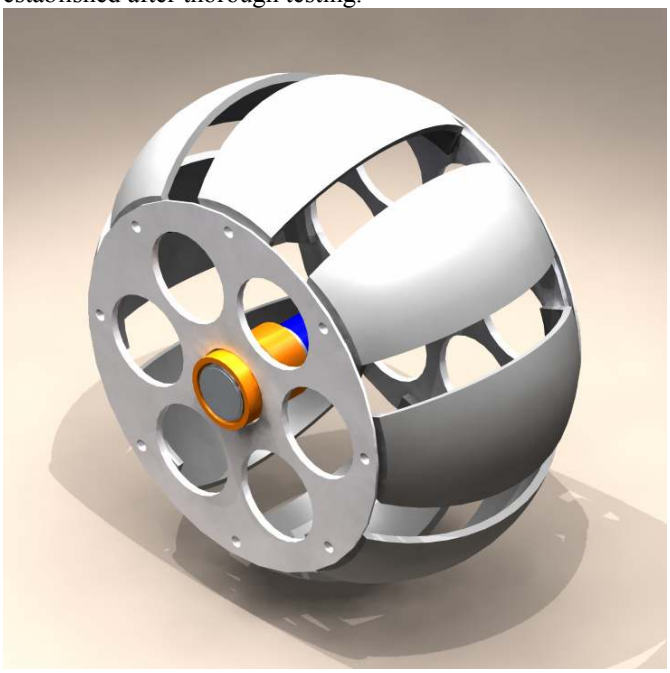

Figure 6: Rendering of the in-wheel motor assembly. The curved tire sections were discarded later since they did not help reduce ground pressure.

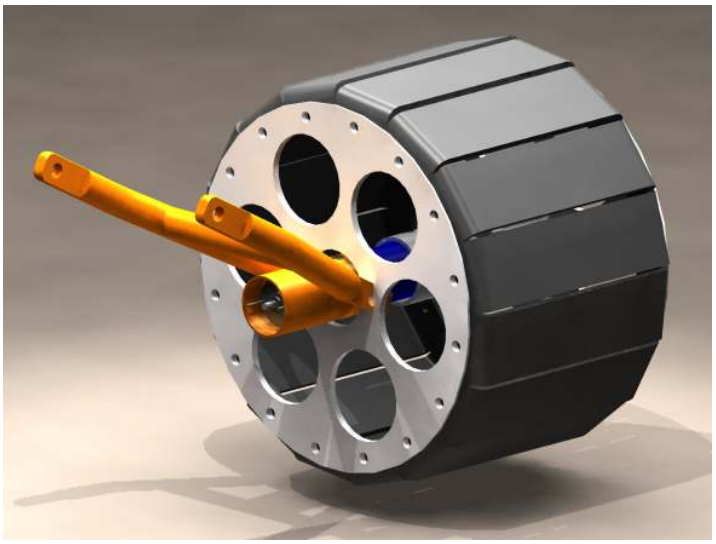

Figure 7: Redesigned wheel mount with 16 sheet metal flats for tires.

A. *Pros*

- Highly fault tolerant with 6 actuators
- Precise motion control
- Lightweight and energy efficient

B. *Cons*

- Complex control system with 6 feedback systems
- Custom wheel fabrication

IV. Future Recommendations

The current drivetrain is self-contained is ready for fabrication for the current robot. However, the following considerations need to be made for drivetrain designs.

1. Establish thorough study parameters so that all aspects of the drivetrain can be modeled as in *Apostolopoulos et al.*
2. Integrate the suspension into the drivetrain, so that the wheel is fully contained system requiring a simple bolting linkage to the main robot body. This provides greater symmetry and repeatability in the fab process.
3. Account for all terrain conditions when choosing motors. Also, incorporate a more robust shaft linkage solution and model using MATLAB/Simulink.

References

[1] Dimitrios S. Apostolopoulos. Analytical Configuration of Wheeled Robotic Locomotion
[2] MER Mission Overview. www.marsinstitute.info
[3] David P. Anderson and Mike Hamilton. Journey Robot. www.geology.smu.edu/~dpa-www/robo/jbot/

V. Appendix A

FAULHABER

DC-Micromotors — 16 mNm

Graphite Commutation

For combination with (overview on page 14-15)
Gearheads:
23/1, 26A, 26/1, 30/1, 38/3
Encoders:
IE2 – 16 ... 512, 5500, 5540

Series 2342 ... CR

		2342 S	006 CR	012 CR	018 CR	024 CR	025 CR	048 CR	
1	Nominal voltage	U_N	6	12	18	24	36	48	Volt
2	Terminal resistance	R	0,40	1,90	4,10	7,10	15,9	31,20	Ω
3	Output power	$P_{2\,max.}$	20,50	17,00	18,10	19,00	19,40	17,70	W
4	Efficiency	$\eta_{max.}$	81	80	81	81	81	81	%
5	No-load speed	n_0	9 000	8 100	8 000	8 500	8 100	8 000	rpm
6	No-load current (with shaft ø 3,0 mm)	I_0	0,170	0,075	0,048	0,038	0,024	0,017	A
7	Stall torque	M_H	87,2	80,0	86,5	85,4	91,4	84,4	mNm
8	Friction torque	M_R	0,98	1,00	0,99	0,99	0,99	0,95	mNm
9	Speed constant	k_n	1 650	713	462	366	231	170	rpm/V
10	Back-EMF constant	k_E	0,604	1,400	2,160	2,730	4,340	5,870	mV/rpm
11	Torque constant	k_M	5,77	13,40	20,70	26,10	41,40	56,10	mNm/A
12	Current constant	k_I	0,173	0,075	0,048	0,038	0,024	0,018	A/mNm
13	Slope of n-M curve	$\Delta n/\Delta M$	103	101	92,5	99,5	88,6	94,8	rpm/mNm
14	Rotor inductance	L	13,5	65	150	265	590	1 050	µH
15	Mechanical time constant	τ_m	6	6	6	6	6	6	ms
16	Rotor inertia	J	5,6	5,7	6,2	5,8	6,5	6,0	gcm²
17	Angular acceleration	$\alpha_{max.}$	160	140	140	150	140	140	10^3rad/s²
18	Thermal resistance	R_{th1} / R_{th2}	3 / 15						K/W
19	Thermal time constant	τ_{w1} / τ_{w2}	6,5 / 490						s
20	Operating temperature range:								
	– motor		– 30 ... + 100						°C
	– rotor, max. permissible		+ 125						°C
21	Shaft bearings		ball bearings, preloaded						
22	Shaft load max.:								
	– with shaft diameter		3,0						mm
	– radial at 3 000 rpm (3 mm from bearing)		20						N
	– axial at 3 000 rpm		2						N
	– axial at standstill		20						N
23	Shaft play:								
	– radial		0,015						mm
	– axial		0						mm
24	Housing material		steel, black coated						
25	Weight		88						g
26	Direction of rotation		clockwise, viewed from the front face						
Recommended values - mathematically independent of each other									
27	Speed up to	$n_{perm.}$	7 000	7 000	7 000	7 000	7 000	7 000	rpm
28	Torque up to	$M_{perm.}$	16	16	16	16	16	16	mNm
29	Current up to (thermal limits)	$I_{perm.}$	2,700	1,400	0,950	0,720	0,480	0,350	A

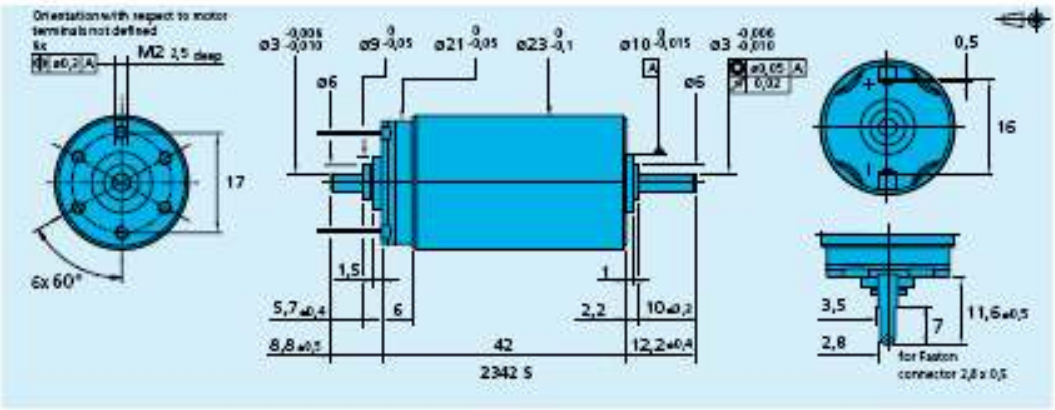

VI. APPENDIX B

Plots of Robot Speed and Torque vs Inclination using 6 Faulhaber 2342 Motors (19W each) for various rolling friction coefficients. Wheel radius = 3".

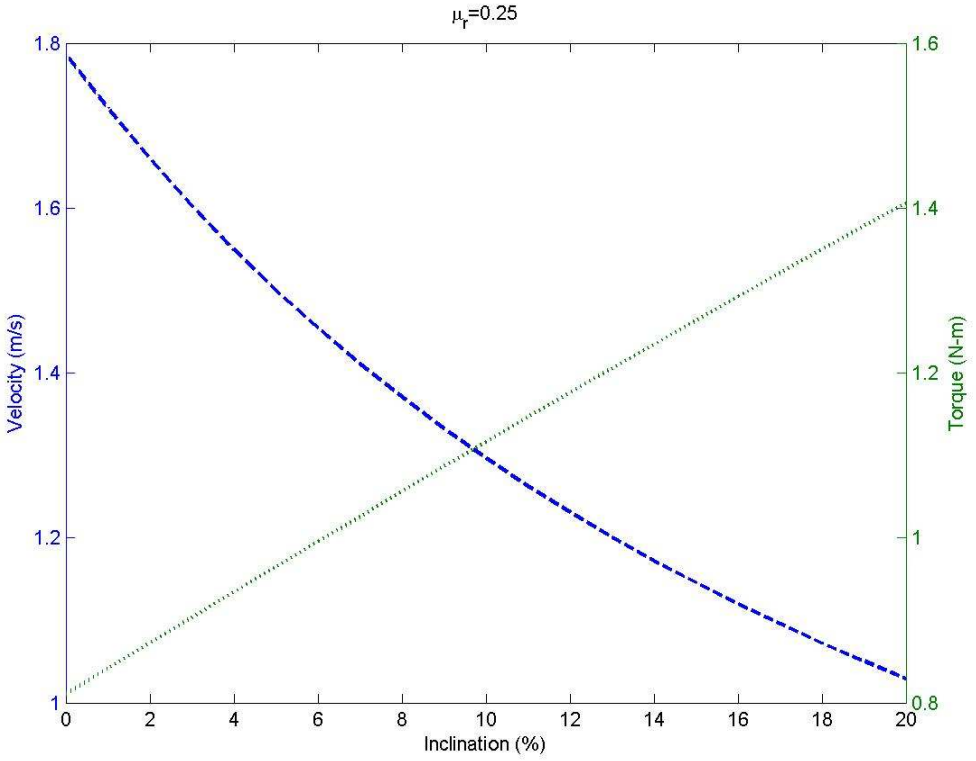

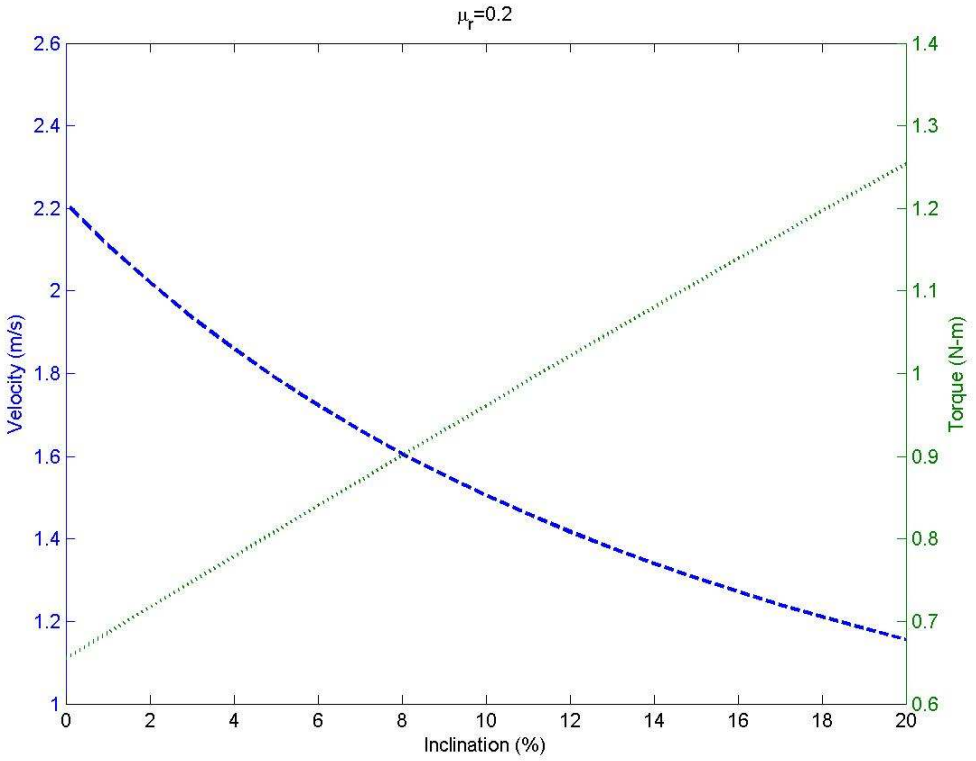

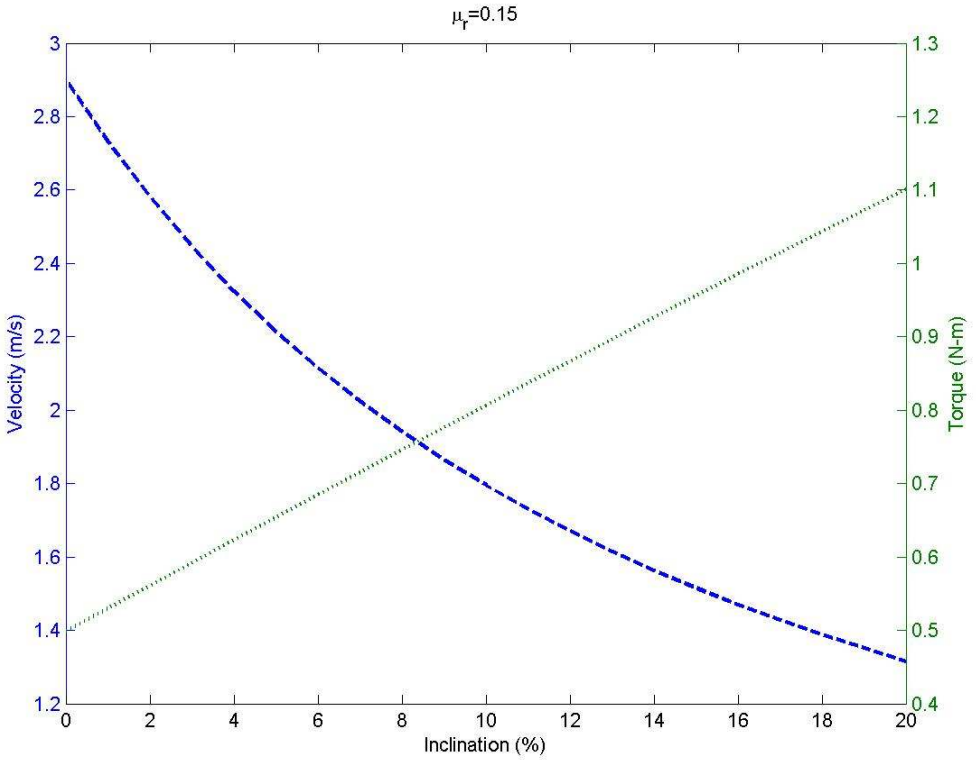
μ_r=0.15
Velocity (m/s)
Torque (N-m)
Inclination (%)
3
2.8
2.6
2.4
2.2
2
1.8
1.6
1.4
1.2
1.3
1.2
1.1
1
0.9
0.8
0.7
0.6
0.5
0.4
0
2
4
6
8
10
12
14
16
18
20

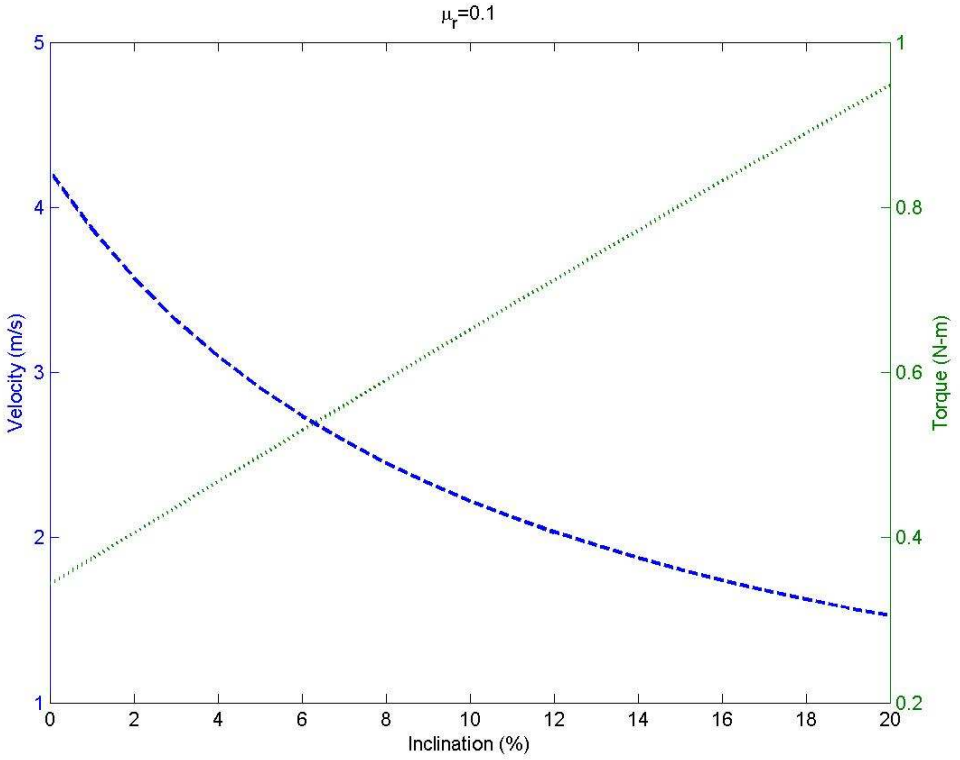
μ_r=0.1
Velocity (m/s)
Torque (N-m)
Inclination (%)
5
4
3
2
1
1
0.8
0.6
0.4
0.2
0
2
4
6
8
10
12
14
16
18
20

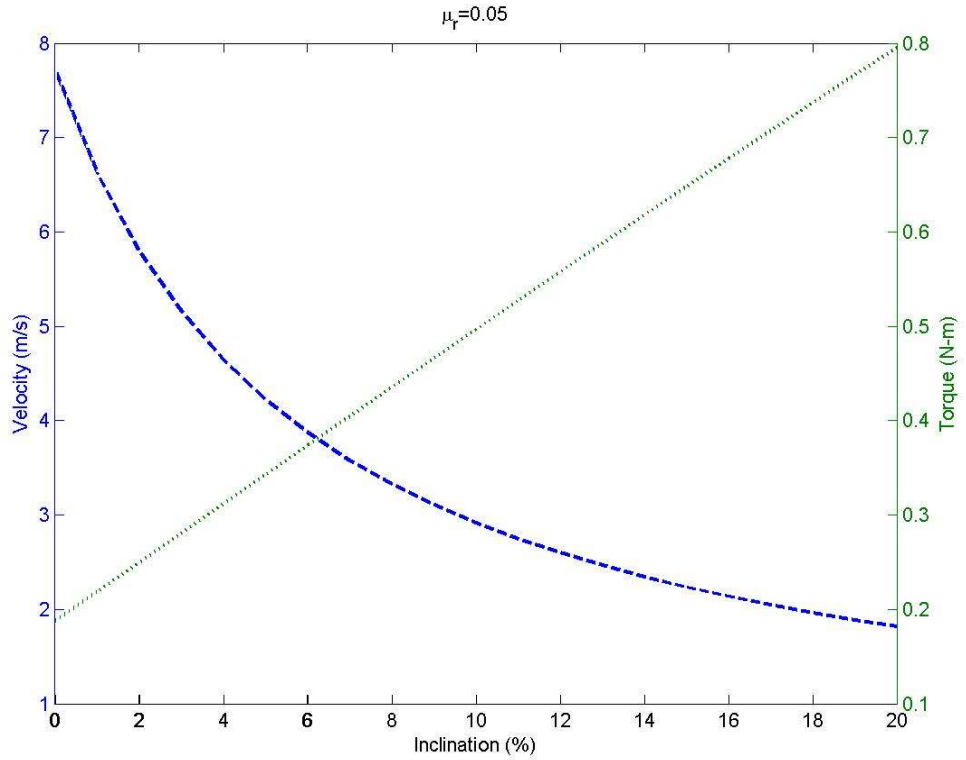
μ_r=0.05
Velocity (m/s)
Torque (N-m)
Inclination (%)
8
7
6
5
4
3
2
1
0.8
0.7
0.6
0.5
0.4
0.3
0.2
0.1
0
2
4
6
8
10
12
14
16
18
20

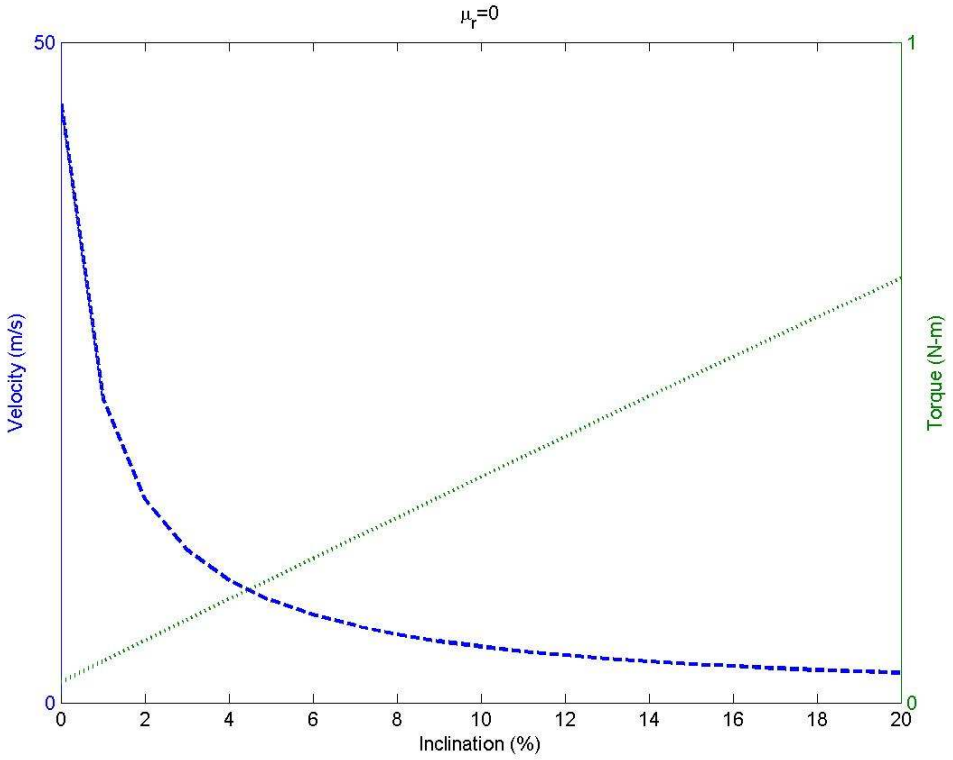
μ_r=0
Velocity (m/s)
Torque (N-m)
Inclination (%)
50
1
0
0
2
4
6
8
10
12
14
16
18
20

Cornell MineSweeper: Sensors (Structure)

Yong Sheng Khoo, Ernie Ko, Franklin Geeng

***Abstract*—the Frame group was to provide an easy solution for mounting the obstacle detection and navigation devices on the vehicle. Besides designing mounting mechanism, the team will also design a protective casing for all above devices. Once built, the electronic devices will be able to withstand outdoor environment such as humidity and heat.**

I. Introduction

THE mechanical team for CU Minesweepers is divided into three main groups to simplify management and separate duties. The drive-train group is responsible for the design of the most efficient way to distribute the motor power to all the wheels. This group will also determine the number of motors for optimum performance. The suspension team is responsible for designing suspension that minimizes the unwanted transmitted motion while moving on uneven surfaces. This report will focus on the frame team which is responsible for the design of the overall frame of the autonomous vehicle. It will also focus on the frame design for the obstacle detection and navigation devices.

The original obstacle detection and navigation devices that were going to be implemented on the vehicle were sonar, lidar, camera, IMU and GPS.

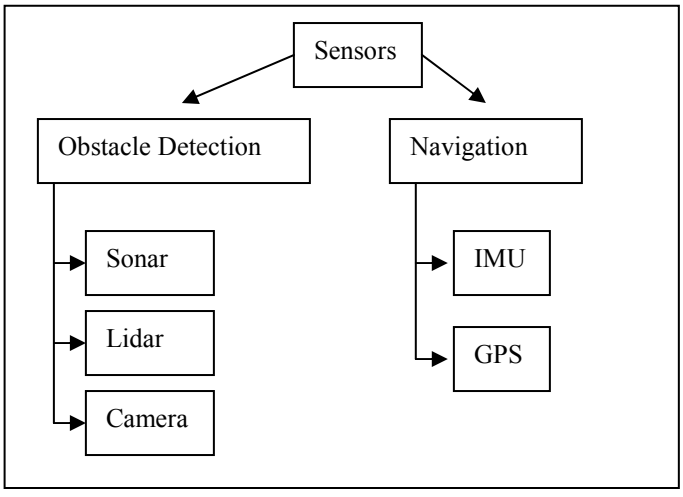

Figure 1: Diagram showing initial obstacle detection and navigation devices that are going to be implemented onboard.

II. Sonar Frame

The first step in designing the mounting device and protective case is to look at the requirements of the sonar.

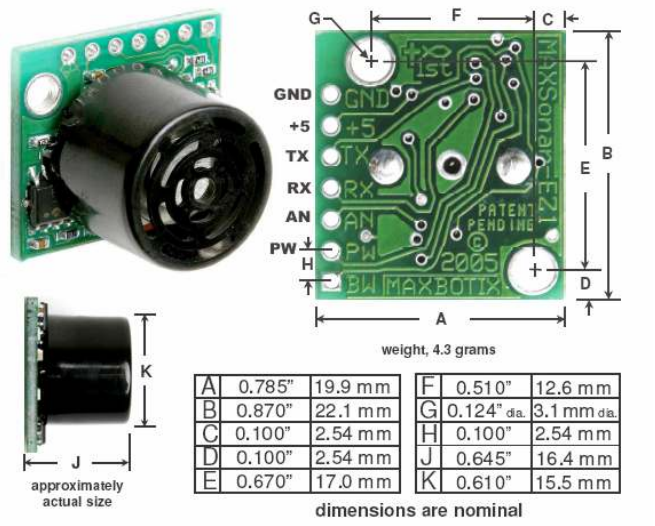

Figure 2: Diagram dimensions of single sonar.

With the sonar chosen, a mounting device needed to be designed to mount the sonar on the vehicle. Some aspects that were considered while designing this part were manufacturability, cost, durability and ease of mounting the device on the vehicle frame. A mounting bracket was chosen for mounting the sonar as it fulfills the requirements needed.

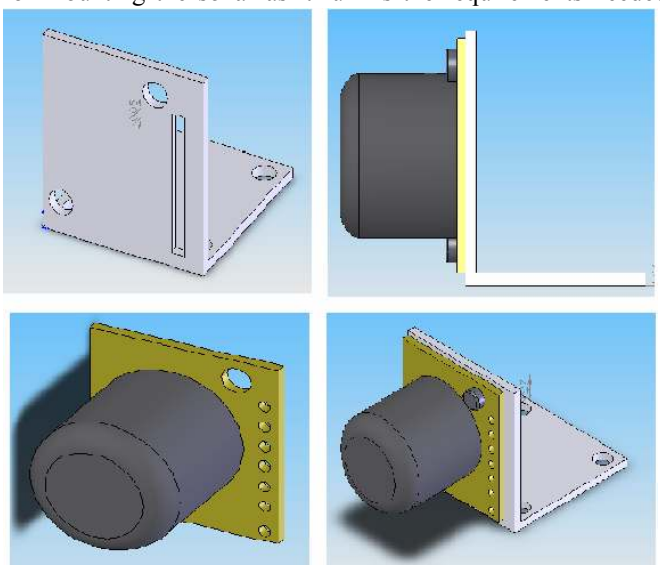

Figure 3: Diagram showing mounting bracket and sonar mounted on it. A simple screw and nuts can be used to fastened sonar to bracket.

As can be seen in Figure 3, each sonar is attached to a single

mounting bracket, which would make sonar arrangements easier. A protective case also must prevent moisture from entering and damaging the electronics on sonar. Since any solid material will block the sonar signal, there must be a hole on the protective case to let the sonar signal pass through. After some testing with the sonar group, it is decided that porous material such as a sponge could be used to cover up the hole to prevent the moisture from entering the protective case and not obstructing the sensing range of the sonar.

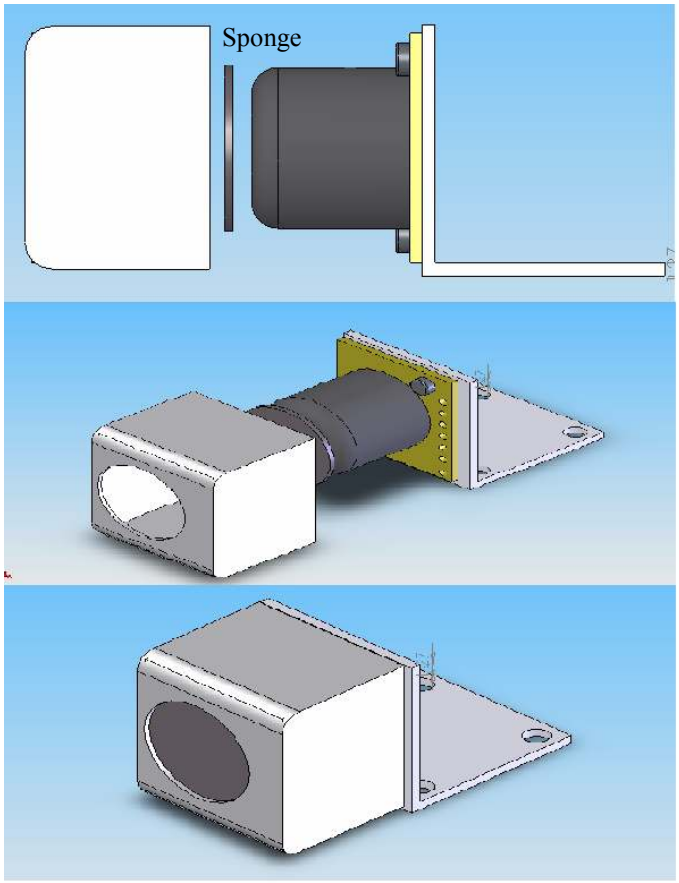

Figure 4: Sonar with protective case

As times passes, the sponge will absorb the moisture until the point that the sonar detecting range is affected. Hence, a clipped on protective case will be used for easy replacement of the sponge. After the wiring at the back is sealed, the sonar will be completely isolated from the outside environment.

III. Camera Mount

The use of cameras as an additional obstacle detection instrument necessitated the design of a corresponding mount that would allow the cameras to maintain a line of sight at a user-adjustable angle with the horizontal axis. To meet these requirements without using motors and the extra current and processing that they would require, the following design was devised.

As Figure 5 shows, the mount assembly consists of a hollow aluminum mast connecting a base, fixed to the top of the robot, and a frame housing a pin about which the actual mount would pivot. The mount would be entirely gravity operated, swinging like a pendulum.

The design of the mount uses attached weights to drive the mount so that it is always normal to the horizontal plane even when the vehicle is moving on an inclined surface. The bolt shown in the figure locks the bar that holds the cameras in place. The user can loosen the bolt to change to a desired angle of the cameras. The rotary damper shown in Figure 6 will be attached to the side of the mount.

Ideally, the mount would pivot about its center of mass, making periodic oscillations from gravity impossible, but friction, tension from any camera cables, and rotary dampers needed to eliminate vibrations during motion require that the mount's center of mass be offset below the pivot point to allow for a driving force at the center of mass.

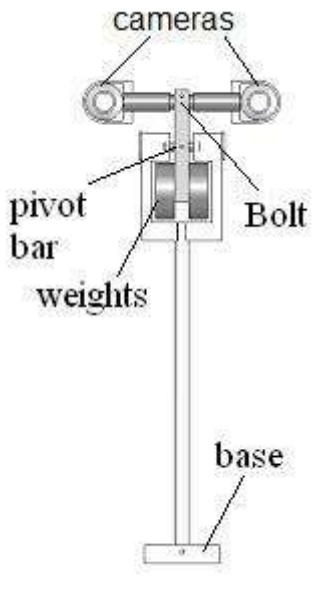

Figure 5: Design of the camera mount assembly (front and isometric views)

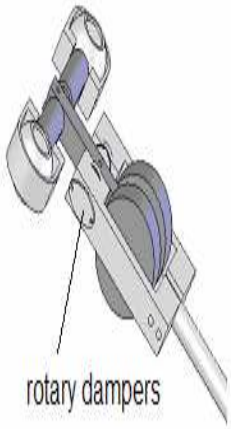

Figure 6: Another view of the camera mount showing the rotary dampers

To allow the mount to accommodate cameras of different weights while still remaining critically damped, the weights were designed to be easily removable and interchangeable via a simple screw connection. Considering the Microsoft webcams depicted in the above figures, dual rotary dampers from mcmaster.com, and the assumption that the initial positions are zero but the initial velocities are non-zero, the following range of critically damped motion was simulated with Matlab.

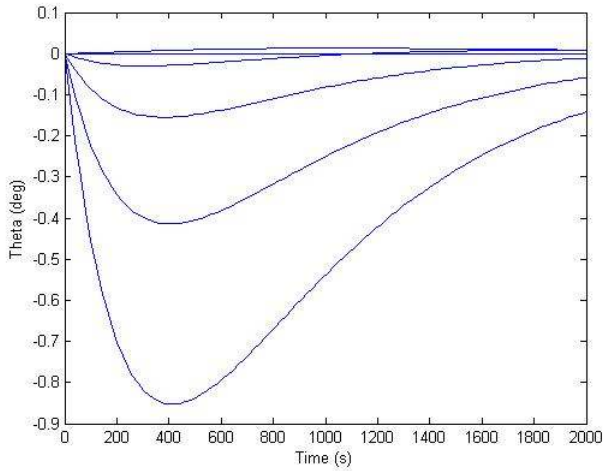

Figure 7: Angle between mount and vertical axis versus time

It should be noted that the initial velocities used were roughly ten times the estimated velocities from the robot traveling at its maximum speed of 2 m/s and much larger than initial velocities caused by vibrations, so the mount can be expected to remain nearly normal during the course of its use.

In addition to having adjustable weights, the mount also features telescoping clamps to actually hold the cameras.

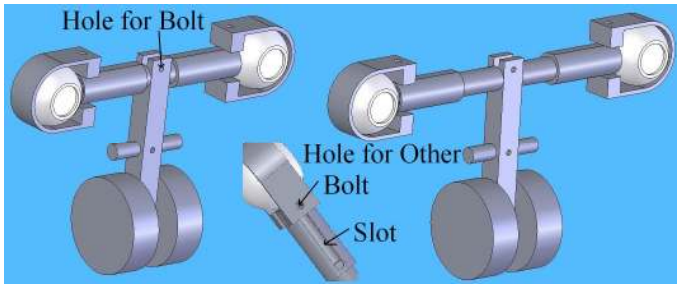

Figure 8: Telescoping clamps

The cameras would be clamped to the ends of slotted sleeves would slide along a bar and be held in place by bolts tightened after adjusting the positions of the sleeves.

IV. LIDAR

A commercially available optical obstacle detection system such as the SICK LMS would cost several thousand dollars too many for Minesweeper's limited budget and ultimate goal of marketing an inexpensive robot. To reduce the cost, the team decided to design simple Lidar that will provide obstacle detection system. A simple SICK LMS can be produced by combining the readily available optical device and servo motor. Figure 9 shows the initial design of the Lidar mount. The main idea behind the design is the rotating servo motor will cause the Lidar device to rotate and mapped out the obstacle in front of the device. This Lidar idea was phased out after the failure of the optical measurement device to work outdoors even with solutions such as filter. The success in the sonar as a obstacle detection device was another reason that focus was shifted away from the Lidar.

Figure 9: Lidar mount design

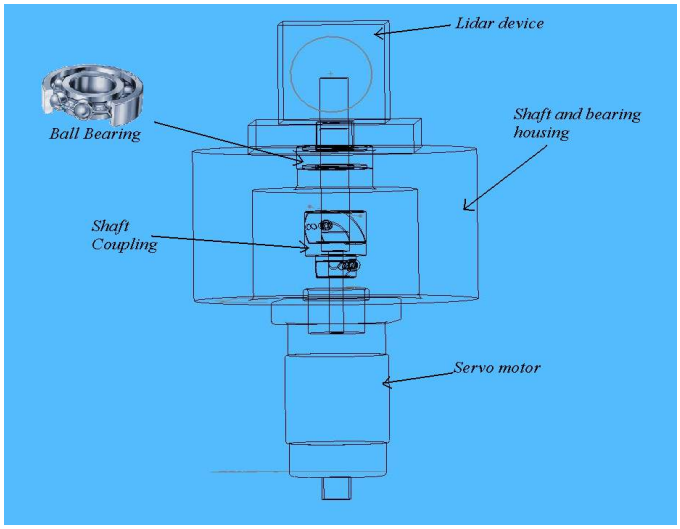

V. IMU AND GPS

Early in the semester, the team acquired an IMU and a GPS. Kionix Company was generous enough to provide the team with a tri-axis accelerometer. In theory, with correct algorithm, the accelerometer can be turned into an IMU. Since further testing is needed for GPS and IMU, the frame design is postponed to next semester.

Cornell MineSweeper: Suspension

Carlos Aguilar, cga9@cornell.edu

I. Suspension Design

A. Introduction

The Mechanical Team had several considerations when designing the suspension for the Cornell Minesweeper. The first role of the suspension is to absorb vibrations which become particularly important with the amount of sensing done by the Cornell Minesweeper. The suspension should also enable the robot to navigate diverse terrains. Mines reside in very harsh terrains so the minesweeper should be able to handle these harsh conditions. Lastly the suspension is one of the most vulnerable components of the robot, so it should be easily reparable or replaceable.

The first minesweeper design had six wheel independent suspension. Inspired by the mars rover, the design was updated this semester to include a rocker bogie system. This system might be the most prominent visual feature of the Cornell Minesweeper and greatly increases the range of different terrains that the robot will be able to navigate.

B. Rocker Bogie System

The Rocker Bogie system contains three wheels per side. There are two sections as can be seen in figure 1. The front section contains one wheel and the connections to the chassis. Attaching the chassis to a single section greatly simplifies the connections and also helps with the clearance of the rear wheels. This front section is attached at a single hinge point to the rear section holds two wheels.

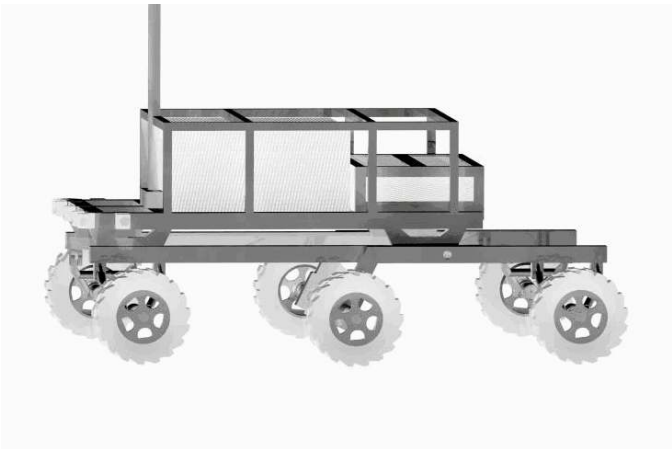

Fig. 1. Rendering of the chassis and drive systems of the Cornell Minesweeper robot.

A modular configuration was also chosen for the minesweeper. Each three wheel system is attached at two points to the robot chassis. This modular design isolates the drive system and allows easy replacement or repair of components in the case of failure due to mine detonation. The modularity also allows for flexibility in the terrain that the robot will be able to navigate. Since the drive system is simply screwed at two points and all electrical connections will be made at a single clip. This means that different drive designs can be manufactured and simply switched in or out to navigate different terrains.

The rocker bogie configuration adds about two pounds per side but allows excellent terrain handling. As can bee seen in figures 2 and 3 each rocker bogie will allow the robot toe conform to terrain and will maximize the power that the wheels deliver.

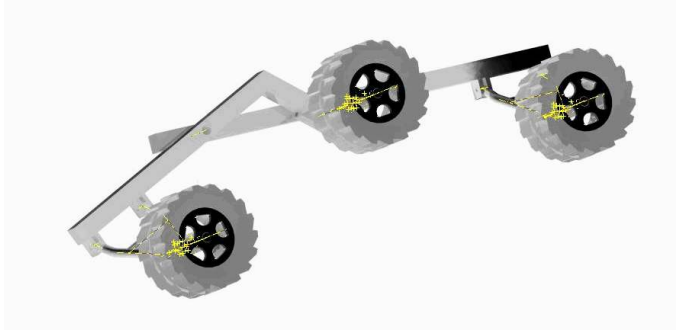

Fig. 2. Example of how the suspension configuration can conform to different terrains. Here the rocker bogie is could be going over a hill-like obstacle.

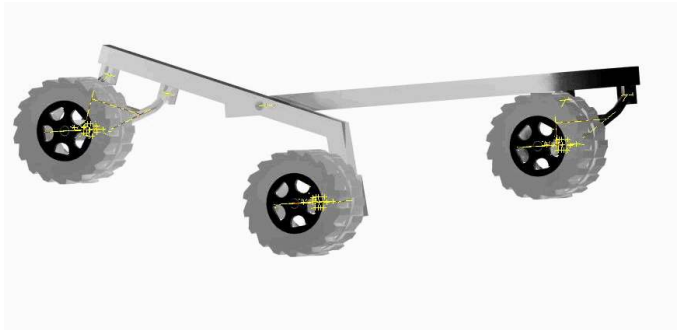

Fig. 3. Here the suspension could conform to a valley-like obstacle.

The design includes three contact points per side at each of the three wheels. Any of these three forces could be producing independent vibrations. To effectively damp these vibrations the robot must have at leas three degrees of freedom. One rotational degree of freedom at the hinge point is inherent in the design. The front and rear wheels are independently suspended in order to allow for the additional degrees of freedom. Linear spring damper systems will be placed on the front and rear wheels and a torsional spring damper will be placed on the hinge.

C. Linkage

Each wheel must be restrained in all three rotational and linear directions. The middle wheel will simply be rigidly

attached to the front of the rear section of the rocker bogie. The other two wheels will be suspended and allowed to move along one line with resistance provided by the linear spring and dampers.

The original design used a ball joint and additional links to steady the wheel in addition to the spring. Since these links do not have reaction moments at the linking points, the twisting in the links was minimized and the majority of the force was uniaxial. This design reduced the twisting of the links and made the forces act along the axes of the links. Ball joints are expensive, however and from the magnitude of the expected forces it became obvious that the design was overbuilt. In the second design a single slanted H-bar was used in addition to the spring. Four pins hold the H-bar in place.

The spring damper system has not yet been selected. This is why it has been omitted from the figures because the setup will be dependent on the selected component's geometries. The simplicity of the H-bar design leaves a lot of space and flexibility in attaching the spring-damper.

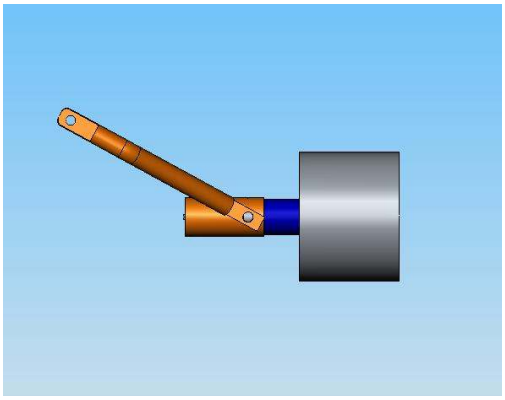

Fig. 4. The H-Bar design from the side.

II. Conclusion

The suspension design is a tried and tested concept and hence is a safe bet for a prototype design. However, this design is not complete and requires specifications such as the spring constants and damping coefficients.

As for future designs, it might be beneficial to incorporate the suspension into the in-wheel motor drivetrain.

Cornell MineSweeper: Structures (Managerial Overview)

John Andersen

As senior leader of the Structures team, I was in charge of delegating tasks and managing the overall goals of the team. I was in charge of representing the team at group meetings and presentations as well as making sure people stayed on task. I also handled the majority of the communications between teams. While I had left the general frame design to Mike, I made sure to take the management lead and maintain a steady flow of information between the group members.

Time line

Building off of our time line from last semester, our main goals for this semester were to have a finalized drive train and suspension system. Other minor goals included begin design a "black box" system to house all internal components, plan and organize sensor mounting positions, and create individual housing cases for each board. We achieved our main goals for the drive train and suspension systems which Mike combined into a frame. We experienced some success with our minor goals. We have sensor positions for all sonar sensors and a design for the camera mount. Sadly, other teams have not finalized electronic boards so designs for the housing units and the black box were unable to continue. Initial design planning has begun for both. This summer fabrication of parts for the suspension, frame, and drive train will begin and continue into the fall. The goal for next semester is to have an assembled frame ready for testing by Thanksgiving.

Design Objectives

The design objectives have been updated from last semester. We are no longer designing two frames but one frame that will fulfill both design requirements. Thus the objectives have been merged and updated as follows:

- All terrain ability – can travel over all different forms of terrain possible to encounter
  - Currently unsure of what types of terrain mine fields are located in – same assumption that the terrain is not perfectly flat – more research needed here but currently will plan to deal with all forms of terrain
- Housing of internal components protects them from environment (i.e. light rain, dirt, moisture, etc.)
- Currently unsure of the weather and physical environment conditions of the mine fields – users will probably expect the robot to function in light rain or moist situations (such as after heavy rain) – will lose clout and respectability if it can only work in perfect weather conditions
- Easy access to the internal components for repairs, removals, and replacements
  - ECE team will probably want easy access to their components – mechanical team should make this as smooth as possible
- Structurally sound – can support weight of all components and payload without failing
  - There is an additional payload for the competition – our structure must be able to handle the weight of itself, the components, and the payload – will need stress tests and identify areas of high stress
- Minimize weight and cost
  - Meant to be used in field operations and to be affordable for those with minefields – must keep costs and weight to a minimum
  - Desire for this to be inexpensive so it will be used – also needs to be easy to replace in event of accident – high chance of accident when working with mines
- It has a low center of gravity to maintain stability
  - Since the terrain will not be flat, the robot must not tip over – complete failure will occur if it tips over – low center of gravity will prevent this possibility
- Marks mine location – physical and electronic (GPS) marking systems
  - GPS location of mine will be useful to removal team but physical mark will be helpful to anyone who might be near mine before removal team arrives – possible marks: paint, flag?
- Survivability - In the event of failure (tips over, structure fails), internal components are salvageable with minimum damage to the components
  - Use of "black box" to protect all internal components in event of failure – more about black box design considerations in next section
- Ability to be located in the event of an accident
  - In event of accident, robot should be easy to locate so as to salvage as much as possible from robot –

methods: homing beacon using GPS, audio device, distress message sent to radio?

- Able to deal with a variety of mines – different sizes, trigger types, etc.
  - Several different times of triggering devices for mines – need to design and plan for as many different types as possible – research needed to identify all types of triggers

- Self navigating – sensor positions?
  - Sensor team has worked with Structure team this semester to identify sensor locations for sonar and cameras
  - Sensor team is doing further research into any other possible sensor needs and best ways to protect sensors

- Simple to use – nothing unnecessarily complex in its operation
  - Retrieval of the data will require an understanding of computing and GPS but operating the robot should not – any soldier or peace keeper should be able to activate, deactivate, recharge/replace battery, etc.

Black Box Design Criteria

As per Prof Garcia's recommendation, we will be researching military specs for black box designs currently in use. This is a top priority next semester but we have down a preliminary criteria list.

Black Box

- Survivability – contains all the vital and expensive electronics of our robot
  - In the event of catastrophic failure, this must be the one thing to survive
  - Possible use of composite materials to protect against shrapnel and heat from exploding mine

- Water proof
  - Since this houses all electronic components, it must be completed water proof
  - Considering use of plastics to cover the walls

- Heat/Temperature Control and Regulation
  - The running electronics will generate heat that can damage them if the heat builds up
  - Environment can also cause internal components to heat up
  - Must have some sort of temperature regulator that will keep electronics cool and prevent overheating – possibly a fan

- Accessibility
  - Must be able to open black box and replace damaged or burnt out boards
  - Accessibility can not allow water to enter black box or other environmental hazards such as dust and dirt

This is only a preliminary criteria list I have generated for the black box. Once more research is completed next semester, we can use and compare the design criteria used by the military for a similar device. The other electronics consideration we made this semester was planning the design for the housing of the boards. We felt the best choice was to make one generic housing design that would be used on all boards. This would make fabrication simpler and simplify the design for the black box. It would also allow for easier replacing and exchanging of boards if such an situation would arise.

Conclusion

The structure team is on course and on time in designing the frame. We are reaching a point that we need more information and communication with other teams. Having finalized the drive train and suspension, the remaining design work to be done is dependent on information from other teams. I found it difficult to get information from any other teams which limited our achievements this semester. In order for this project to remain as successful as it has been, there needs to be more communication between the different teams.

Cornell MineSweeper: Frame

Mike Nagele, *Member, FDIC*

At the beginning of the semester, I was again tasked with the responsibility of designing the frame for the mechanical team. To start designing this frame, I based the initial parameters off of the work done last semester on the temporary frame. This involved utilizing the morphological charts, dimensions, and material selection processes.

For expense and ease of use, I chose 1 inch square aluminum 6061-T6 tubing as the main structural component of the frame. This would be light and cheap, while the additional time over the summer and next semester would allow for the necessary time to properly assemble the components into the design.

Since all of the primary components of the minesweeper frame were designed independently, the initial design of the frame was a simple rectangular prism as shown in Figure 1.1.

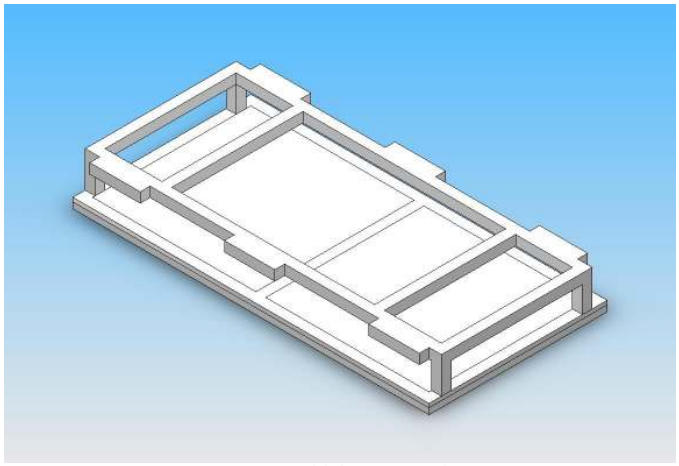

Figure 1.1: Initial Frame Design

As a rough design, the frame depicted is not designed for manufacturability; however, small modifications were made to incorporate it with the initial suspension. Pieces were expanded to provide attachment points for the independent wheel suspension. Additionally, the electronics were placed in a rack designed around the batteries and motors in located within the interior cavity of the frame.

Once a rough model of the robot was designed with all the components created by individuals brought into one design, we performed a design review that looked at the interaction of all the systems and what components could be made better, more efficient, lighter, and which parts needed to be redesigned completely. Looking at the suspension design, I realized I could increase the ground clearance of the robot while making the frame lighter and redistributing the forces applied in the frame. Additionally, more members were brought into the mechanical team to help design the sensor attachments, electronics mounting, and several other details allowing me to focus on the primary structure of the robot.

When redesigning the frame for the robot, I tried to increase the maximum ground clearance possible in the middle of the robot. I also focused on making a design that distributed the forces due to static loading into the box aluminum as bending stresses in order to utilize the stiffness benefits of the material selected. The results are shown in Figure 1.2, which shows the frame structure as well as connection points for the lower contact of the individual suspensions for the 6 wheels of the robot. While the model is incomplete, it weighed over 13 pounds and still needed more work to properly attach the bottom supports to the top part of the frame. The design process was stopped before the finishing touches could be added which accounts for the fact that the interior of some of the aluminum tubing is visible.

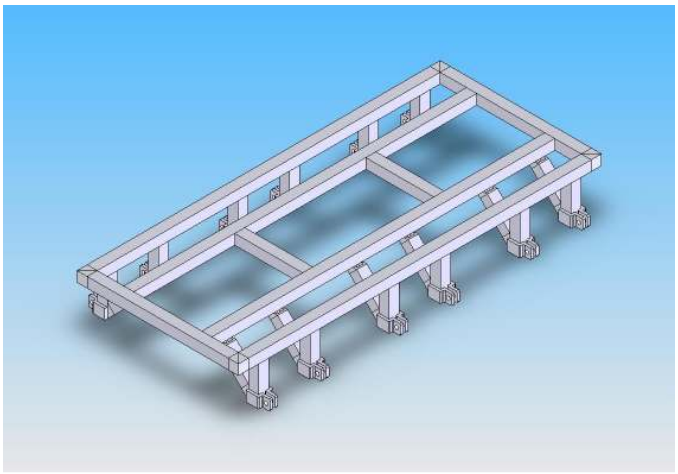

Figure 1.2: Preliminary Redesign of Frame

Work on the frame had to stop and restart because suspension was redesigned during this process. It went from 6 individually suspended wheels to the bar supported suspension discussed in this report. My work on the frame needed to be changed because this new suspension had very different methods of connecting to the frame.

To accommodate the change in suspension, I kept the basic design of the frame the same: a one layer rectangle composed 1 inch box aluminum. The frame length was reduced to align with the suspension dimensions, allowing the wheels to perform optimally without interference of the frame on the terrain being traversed. In order to reduce the stress concentrations in the

frame, small brackets made from a solid aluminum block were made to attach the frame to the suspension. These brackets apply distributed loads on the frame rather than point loading.

The remodeled system both increases the center clearance height of the robot, but also reduces the weight of the frame. With the bar suspension system, there was more rigidity in the suspension subsystem itself eliminating some of the rigidity requirements of the frame. After a lengthy redesign process, the frame created is shown in Figure 1.3.

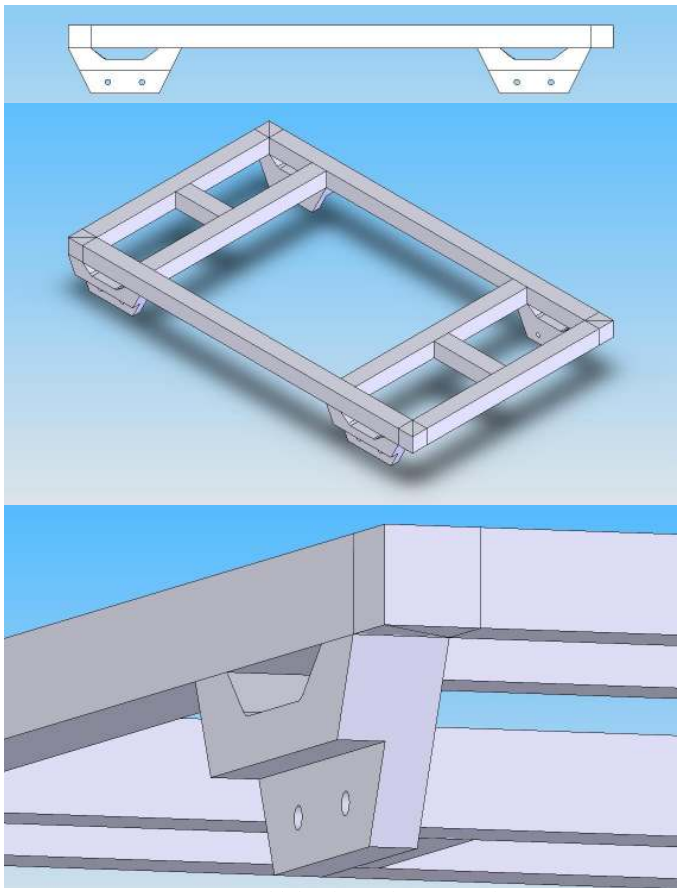

Figure 1.3: Multiple Views of Frame Design

This new frame design increases the benefits of the earlier design from Figure 1.2. The weight of the frame was reduced to 6.438 pounds, and the ground clearance in the center of the robot was increased to 8 inches. I then took this model and imported it into ANSYS to look at how the frame would react to the static loading, which is the primary function of the frame. Loading conditions were modeled as a 14 pound load applied to the back of the frame representing the weight of the batteries. An additional 150 pounds were applied to the sides of the frame to model the weight of payload and the rest of the robot. This weight of the robot will most likely be spread throughout the frame more uniformly, but by modeling the weight in this manner, the worst case scenario is analyzed. The bottoms of the suspension mounting brackets were fixed in space to represent the support of the suspension and wheels.

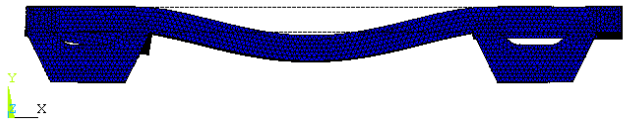

Figure 1.4: Displacement Results of ANSYS Analysis

Results from this analysis are highlighted in Figures 1.4 and 1.5. Static loading created a maximum deflection of X.XX inches in the center of the sides, which is what was expected. The maximum and minimum Von Mises stresses are 477 psi and -585 psi respectively. Comparing this to an elastic limit of 27 ksi for 6061-T6 aluminum, and the designed frame is well within the safety range, safety factor of 46. More components can be added to the frame to add rigidity or attachment points for other components of the robot; however, any additions to the frame do not need to be structural.

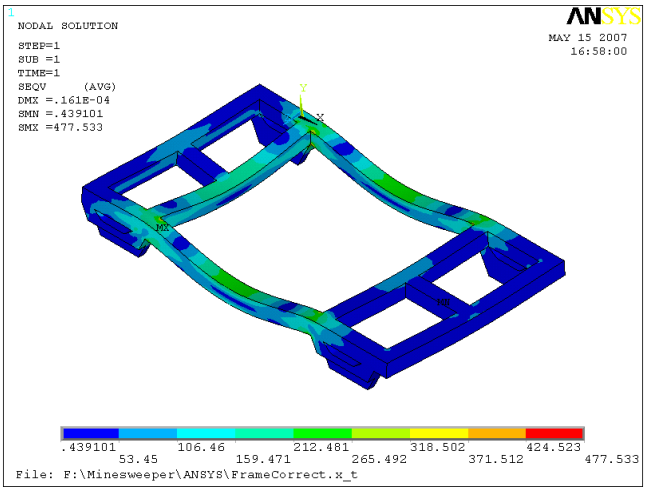

Figure 1.5: Von Mises Stress Distribution